



Seasonal, Interannual, and Longitudinal Patterns in Estuarine Metabolism Derived from Diel Oxygen Data Using Multiple Computational Approaches

Spencer J. Tassone¹ · Paul A. Bukaveckas¹

Received: 15 August 2018 / Revised: 15 January 2019 / Accepted: 18 January 2019 / Published online: 12 February 2019
© Coastal and Estuarine Research Federation 2019

Abstract

Twenty-three station-years of diel oxygen data for the James River Estuary were analyzed to characterize longitudinal, seasonal, and interannual patterns of gross primary production (GPP) and ecosystem respiration (ER). We compared two commonly used methods for deriving metabolism (bookkeeping and Bayesian) to determine whether the observed patterns were robust with respect to computational methodology. The two methods revealed similar longitudinal patterns of increasing GPP and ER, and decreasing net ecosystem metabolism (NEM), with increasing salinity. Seasonal patterns in GPP and ER tracked water temperature and solar radiation, except during high discharge events when metabolism declined by 40%. The bookkeeping method yielded higher estimates of GPP and ER in the higher end of the range, and smaller estimates in the low end of the range, thereby accentuating seasonal and longitudinal differences. Inferences regarding net autotrophy and heterotrophy were robust, as both methods yielded positive estimates of NEM at the chlorophyll maximum (tidal fresh segment) and negative values for the saline portion of the estuary. Inferences regarding the relative importance of allochthonous inputs (based on inferred ER at GPP = 0) differed between the two methods. Values derived by the bookkeeping method indicated that respiration was largely supported by autochthonous production, whereas the Bayesian results indicated that autochthonous and allochthonous inputs were equally important. Overall, our findings show that methodological differences were small in the context of longitudinal, seasonal, and interannual variation but that the bookkeeping method yielded a wider range of values for GPP and ER relative to the Bayesian estimates.

Keywords Production · Respiration · Metabolism · Bayesian · Chesapeake Bay

Introduction

Ecosystem ecologists have long been interested in primary production because of the important role that primary producers play in elemental cycles and food web energetics (Lindeman 1942; Odum 1956). Recent interest in this topic has sought to place gross primary production (GPP) in the broader context of ecosystem metabolism, i.e., the balance between organic matter (OM) production via photosynthesis and OM consumption via autotrophic and heterotrophic respiration (ecosystem respiration; hereafter, ER). In aquatic systems, interest in net ecosystem metabolism (NEM = GPP –

ER) has reflected in part a desire to understand the role of subsidies (allochthonous OM inputs) in supporting ecosystem respiration and to characterize aquatic systems as being sources or sinks in the context of the global carbon cycle (i.e., net autotrophic (GPP > ER) or heterotrophic (ER > GPP); Vannote et al. 1980; Borges 2005; Tranvik et al. 2009; Raymond et al. 2013; Herrmann et al. 2015; Houser et al. 2015; Hall et al. 2016). Interest in aquatic ecosystem metabolism has also been fueled by technological advances in autonomous monitoring of dissolved oxygen (DO), which allow for characterization of ecosystem metabolism over larger spatial and temporal scales, and by computational advances in the means by which these data are analyzed (Grace et al. 2015; Hall et al. 2016; Winslow et al. 2016; Bernhardt et al. 2018).

Computational methods vary in their complexity and in the variety of parameters needed to derive ecosystem metabolism estimates. A commonly used method is the “bookkeeping” approach, which tracks incremental changes in DO at night

Communicated by: James L. Pinckney

✉ Paul A. Bukaveckas
pabukaveckas@vcu.edu

¹ Department of Biology and Center for Environmental Studies, Virginia Commonwealth University, Richmond, VA, USA

to estimate ER and during the day to estimate net ecosystem production (NEP) and GPP (from daytime NEP plus daily ER). Caffrey (2003, 2004) used this method to analyze diel oxygen data from 42 estuaries that were part of the National Estuarine Research Reserve System (NERRS). A key challenge to deriving open system estimates of metabolism is properly accounting for non-biological oxygen fluxes, which include atmospheric exchange (hereafter, AE) and advective oxygen fluxes. AE is regulated by the concentration gradient between air and water (i.e., dissolved oxygen saturation) and by the gas transfer velocity. The former is easily measured, whereas the latter is difficult to measure, and often modeled based on wind speed and water velocity (Deacon 1981; Wanninkhof 1992; Hopkinson and Smith 2005; Holtgrieve et al. 2010; Raymond et al. 2012). Within estuaries, there is a complex interaction of factors affecting non-biological oxygen fluxes including tidal forces (which reflect tidal amplitude and channel morphometry), fluvial forces (which vary longitudinally and with discharge), and wind-driven mixing forces (which are influenced by fetch and atmospheric conditions; Raymond and Cole 2001; Ho et al. 2011; Crosswell et al. 2012). For the NERRS analysis, AE was calculated from the air-water concentration gradient and a fixed exchange coefficient. An advantage of this approach is that it requires minimal parameterization (e.g., in the absence of data on wind and water velocity), and it has been applied to a large number of estuaries, thereby facilitating cross-system comparisons.

Bayesian analyses are a useful alternative to the bookkeeping approach as they offer uncertainty estimates for modeled parameters (GPP and ER) inclusive of observation uncertainty (measurement precision and accuracy), process uncertainty (stochasticity of model parameters), and model uncertainty. This approach readily accommodates variable rates of atmospheric exchange arising from differences in wind, fluvial, and tidal forcing (Solomon et al. 2013; Hall et al. 2016; Winslow et al. 2016). By this method, unmeasured parameters (i.e., GPP, ER, AE) and associated parameter uncertainty are treated as random variables with prior information (hereafter, priors) regarding their distributions (Holtgrieve et al. 2010; Grace et al. 2015; Hall et al. 2016; Winslow et al. 2016). Bayesian analyses are computationally intensive and require prior information about the system as well as ancillary data to model atmospheric exchange (Grace et al. 2015; Winslow et al. 2016). While both the bookkeeping and Bayesian methods use the same input data (diel oxygen measurements), they differ in the computational methods used to parameterize metabolic rates (arithmetic vs. conditional probabilities). Ideally, inferences about spatial and seasonal patterns in estuarine metabolism should be robust with respect to the methods used to derive GPP and ER, though we know of no prior studies that have directly compared outcomes from these computational approaches.

We analyzed diel oxygen data from the James River Estuary using bookkeeping and Bayesian methods to

determine whether inferences about seasonal, interannual, and longitudinal patterns in metabolism were sensitive to computational methodology. Relationships between metabolic estimates derived using both methods were used to test relationships with pelagic metabolism, solar radiation, and water temperature and to make inferences about sources of OM supporting metabolism. Results from these analyses were used to address two questions: (1) How does GPP, ER, and NEM vary seasonally, interannually, longitudinally, and in response to high discharge events? and (2) Is our assessment of temporal and spatial patterns in GPP, ER, and NEM sensitive to the computational methods used to derive these terms?

Methods and Materials

Study Site

The James River is the third largest and southern most of the five major tributaries of Chesapeake Bay. It drains a mountainous catchment (watershed area = 26,101 km²) comprised of 67% forest, 20% agriculture, 12% urban, and 1% wetland (Bricker et al. 2007). The James River has a total length of 545 km, of which the lower third is tidal extending from the Fall Line in Richmond, VA to the confluence with Chesapeake Bay (Fig. 1). The James River Estuary (JRE) is divided into segments based on salinity: tidal fresh (TF, < 0.5 ppt), oligohaline (OH, 0.5–5 ppt), mesohaline (MH, 5–18 ppt), and polyhaline (PH, > 18 ppt; USEPA Chesapeake Bay Program Office 2005). The TF segment is further divided into upper and lower segments which differ in their geomorphology. The upper TF segment, located between the Fall Line and the confluence with the Appomattox River, has a riverine morphometry with a deep (> 3 m), constricted channel and low ratio of photic depth to total depth (Bukaveckas et al. 2011; Wood and Bukaveckas 2014). The lower TF section extends to the Chickahominy River and is characterized by a more estuarine morphometry, with shallow (< 3 m) depths, a broader channel, and more favorable light conditions (Bukaveckas et al. 2011; Wood and Bukaveckas 2014).

Ecosystem Metabolism

Daily rates of ecosystem GPP, ER, and AE were derived using the single-station open-water method. We analyzed 23 station-years of continuous oxygen monitoring data to assess seasonal, interannual, and longitudinal patterns in estuarine metabolism. The Virginia Estuarine and Coastal Observing System (VECOS) dataset obtained from the Virginia Institute of Marine Science included 15-min oxygen measurements recorded from March to November during 2006–2008 at stations located in each of the five salinity segments (Table 1). An additional 8 years of data (2009–2016) were available

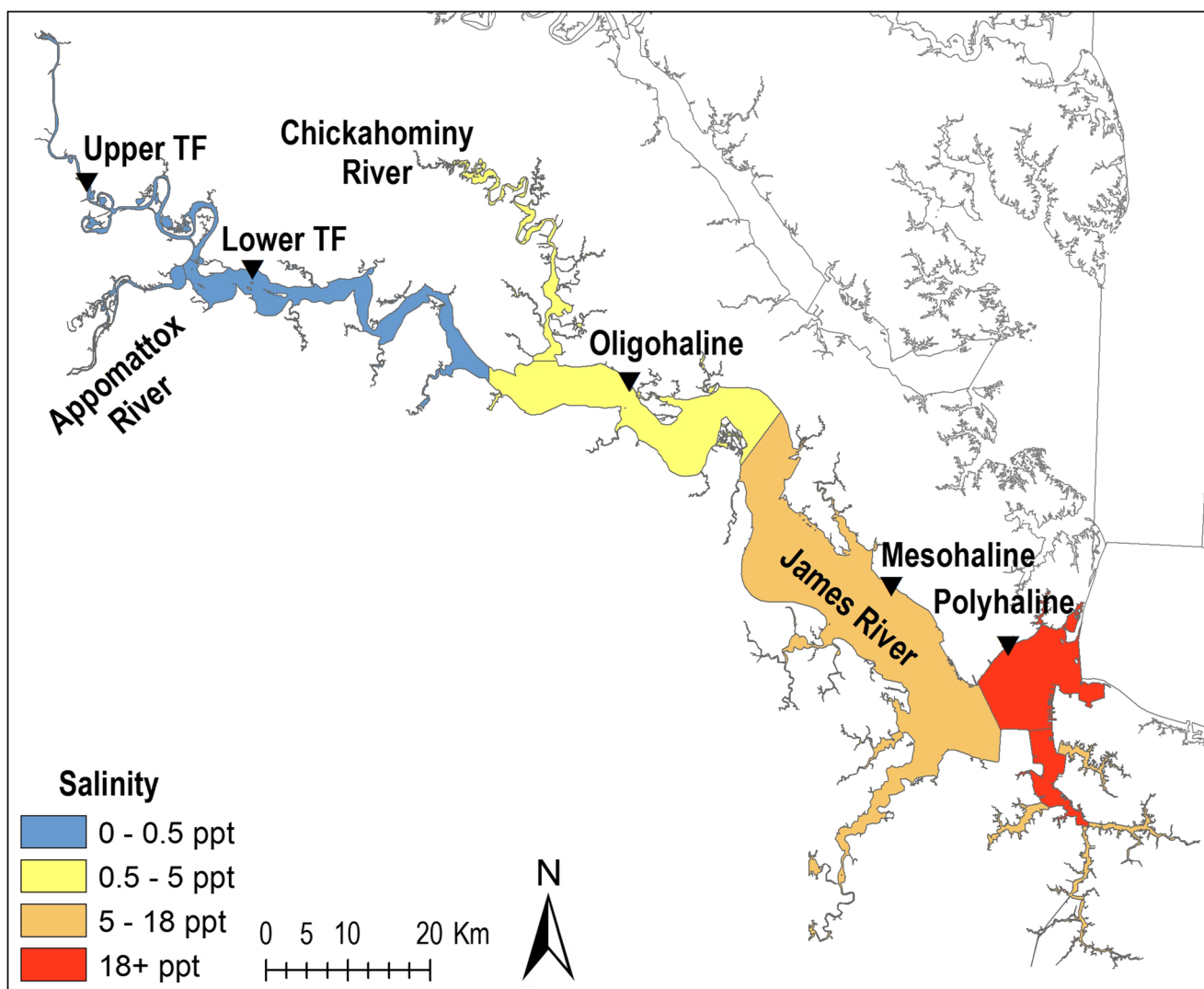


Fig. 1 Salinity zones and locations of continuous monitoring sites (black triangles) within the James River Estuary

from one of these stations (Virginia Commonwealth University Rice Rivers Center Research Pier) and included 15-min oxygen measurements recorded year-round. All data were collected with optical oxygen probes using YSI 6600 water quality sondes (2006–2014) or YSI EXO2 water quality sondes (2015–2016). Sondes were calibrated every 3 weeks. An important assumption when determining metabolic rates using the single-station method is that local DO concentrations are not influenced by advective oxygen fluxes (i.e., tidal stage; Cole et al. 2000; Caffrey 2003). To test for advective influences, we analyzed dissolved oxygen concentrations from the longitudinal (VECOS) dataset using General Additive Models (GAMs; Morton and Henderson 2008; Richards et al. 2013). The GAM approach allowed us to quantify segment-specific functional relationships between dissolved oxygen concentrations and water elevation (tidal stage) along with time of day (solar effects) and water temperature (seasonal effects).

Bookkeeping Method

Following Caffrey (2003, 2004), 15-min DO measurements (g m^{-3}) were smoothed to 30-min averages and multiplied by water depth (m) to obtain areal rates of oxygen flux, which were summed across 24-h periods ($\text{g O}_2 \text{ m}^{-2} \text{ day}^{-1}$; Eq. 1).

$$\text{O}_2 \text{ flux} = (\text{DO}_{t2} - \text{DO}_{t1}) \times \text{Water depth} - \text{AE} \quad (1)$$

For this analysis, a fixed segment-specific mean depth was used (i.e., without consideration for seasonal and tidal variation in water surface elevation; see Table 1).

AE was derived based on DO measurements (as % saturation) and a fixed gas transfer coefficient ($0.5 \text{ g O}_2 \text{ m}^{-2} \text{ h}^{-1}$; Eq. 2). This assumes that AE is affected solely by the air-water concentration gradient and thus varies between -0.5 to $0.5 \text{ g O}_2 \text{ m}^{-2} \text{ h}^{-1}$ when water column saturation is between 0 and 200%. Though the bookkeeping method can be adapted to

Table 1 Site characteristics of continuous monitoring locations in the James River Estuary

Segment	Salinity (ppt) Mean ± SD	Area (km ²)	Mean depth (m)	Site name	Distance (rkm)	Collection years	
						VECOS	VCU
Upper tidal fresh	0.1 ± 0.1	21	2.7	Osborne Landing	159	2006–2008	–
Lower tidal fresh	0.1 ± 0.1	82 ^a	2.5	Rice Rivers Center	119	2006–2008	2009–2016
Oligohaline	2.8 ± 2.5	156 ^b	3.1	4H Camp	71	2006–2008	–
Mesohaline	15.3 ± 4.0	331 ^c	3.1	James River Country Club	29	2006–2008	–
Polyhaline	20.1 ± 3.0	98 ^d	5.6	Wythe Point	4	2006–2008	–

Based on Chesapeake Bay Program segmentation scheme. Link to segmentation salinity ArcMap GIS layers can be found using the following link: <https://usgs.maps.arcgis.com/home/item.html?id=d96647aad2894d2e874cb4a9189f4c4b>. Segment areas are from the Chesapeake Bay Program, and salinity data are from the VECOS dataset

^a Lower TF segment included tidal fresh section of the Appomattox River

^b Oligohaline segment included oligohaline segment of Chickahominy River

^c Mesohaline segment included mesohaline segments of the Lafayette River and the eastern, southern, and western branches of the Elizabeth River

^d Polyhaline segment included the polyhaline segment of the Elizabeth River

accommodate the effects of variable wind and water speed on atmospheric exchange (Staeher et al. 2012; Collins et al. 2013), we chose the simpler formulation to compare against the Bayesian results.

$$AE = \left(1 - \frac{DO_{sat,t_2} + DO_{sat,t_1}}{200} \right) \times 0.5 \times \Delta t \quad (2)$$

DO fluxes during daylight hours were considered NEP, while ER was derived by extrapolating nightly O₂ fluxes to a 24-h period. GPP was derived based on the sum of NEP + ER during daylight hours, and NEM was derived by subtracting daily ER from GPP.

Bayesian Method

The program “streamMetabolizer” (version 0.10.7; Appling et al. 2017; R Core Team 2017) uses a Bayesian approach for inverse modeling, which fits a numerical model describing oxygen gains and losses to input data (e.g., DO measurements). The Bayesian model derives unmeasured metabolic parameters (θ ; i.e., GPP and ER) using a known prior probability ($P(\theta)$) distribution (mean and SD) of θ and a vector of measured input parameters (D ; i.e., DO concentration, DO saturation, day length, and depth; Eq. 3; Hobbs and Hooten 2015, Hall et al. 2016). The likelihood ($P(D|\theta)$) of the measured input data given prior estimates of θ is proportional to the posterior distribution [$P(\theta|D)$] of θ from which estimates of our unmeasured metabolic parameters are derived.

$$P(\theta|D) \propto P(D|\theta) \times P(\theta) \quad (3)$$

The Bayesian analysis was performed using estuarine-specific priors for GPP and ER, site-specific priors for AE, and locally measured tidal variation in depth. Tidal variation in depth was determined from sonde measurements collected

in conjunction with DO data. Priors for GPP and ER are available via streamMetabolizer, but these are generic values (not estuarine-specific) representing previous applications, many of which were small stream studies. We derived estuarine-specific priors using previously published data from six Mid-Atlantic estuaries (Caffrey 2004). From this dataset, we selected years for which at least 9 months of data were available and derived the mean and standard deviation of GPP ($\mu = 6.6 \text{ g O}_2 \text{ m}^{-2} \text{ day}^{-1}$, $\sigma = 9.8 \text{ g O}_2 \text{ m}^{-2} \text{ day}^{-1}$) and ER ($\mu = 8.1 \text{ g O}_2 \text{ m}^{-2} \text{ day}^{-1}$, $\sigma = 10.2 \text{ g O}_2 \text{ m}^{-2} \text{ day}^{-1}$). To obtain segment-specific estimates of AE, we used output from the James River hydrodynamic model (Shen et al. 2016). This model uses an additive combination of the effects of wind speed (Thomann and Mueller 1987) and water velocity (O'Connor and Dobbins 1958) to derive the gas transfer velocity (k_{O_2} ; m day^{-1}). Wind speed data were obtained from the Richmond and Norfolk airports. AE was derived for each 15-min measurement as k_{O_2} multiplied by the difference between DO saturation and modeled DO. Model derived k_{O_2} values averaged 1.12, 1.48, 1.05, 1.67, and 1.33 m day^{-1} for the upper and lower TF, OH, MH, and PH segments, respectively. Site-specific k_{600} priors were derived by normalizing the temperature-dependent Schmidt number (Sc_{O_2}), which relates gas solubility to water viscosity in flowing freshwater ecosystems to 600 and to 660 in saline ecosystems (Wanninkhof 1992; Raymond et al. 2012). The normalized Sc_{O_2} is then raised to the power of -0.5 due to wind-induced surface water turbulence (Jähne et al. 1987) and multiplied by the segment-specific average k_{O_2} (Eq. 4, Raymond et al. 2012).

$$k_{600} = (600/Sc_{O_2})^{-0.5} \times k_{O_2} \quad (4)$$

Segment-specific k_{600} priors were 0.95 ± 0.14 (upper TF), 1.33 ± 0.23 (lower TF), 0.92 ± 0.13 (OH), 1.49 ± 0.22 (MH), and $1.27 \pm 0.23 \text{ m day}^{-1}$ (PH).

Pelagic Metabolism

Pelagic production and respiration were measured to determine their relative contributions to ecosystem production and respiration. Light and dark bottle incubations were performed over an annual cycle during 2015–2016 at a station located in the lower tidal fresh segment (VCU Rice Pier). Surface water samples were collected twice per month when water temperatures were > 10 °C and once per month when water temperatures were < 10 °C (total = 26). Light and dark bottles were incubated for 2 and 24 h, respectively. Preliminary experiments showed non-linear effects (reduced hourly rates of metabolism) when incubation lengths in light bottles exceeded 2 h. Triplicate light bottles (60 mL BOD) were incubated at 0.5-m depth intervals within the photic zone (0–2.0 m). DO concentrations were measured using the micro-Winkler technique to obtain a precision ~ 0.01 mg O₂ L⁻¹ (Carignan et al. 1998; Bukaveckas et al. 2011). The change in DO from the start to the end of the incubation was used to determine net pelagic production (NPP; light bottles), R (dark bottles), and GPP (as NPP + R). Hourly rates were extrapolated to daily values based on the proportion of incident solar radiation occurring within the time span of the incubation. Solar radiation data were obtained from the NERRS Taskinas Creek station, located 45 km from the VCU Rice Center pier. Daily rates of pelagic GPP and R were compared to ecosystem values derived by bookkeeping and Bayesian methods for corresponding dates. Annualized estimates of pelagic GPP and R were also compared with annual ecosystem values for the lower tidal fresh time series dataset.

Ancillary Data and Statistics

To characterize longitudinal gradients in the James River Estuary, we used monthly monitoring data collected by the Chesapeake Bay Program (salinity, chlorophyll-*a*, Secchi depth, TSS, TN, and TP) for the period during which diel oxygen data were available (March–November 2007–2009; <http://datahub.chesapeakebay.net/WaterQuality>). We also obtained estimates of areal coverage by submersed aquatic vegetation (SAV) for corresponding years (<http://web.vims.edu/bio/sav/index.html>). To assess the effects of high discharge events on metabolism in the upper estuary (tidal fresh segment), we used discharge data from USGS gauges located at the Fall Line of the James and Appomattox Rivers. We calculated the average discharge, GPP, and ER during events (i.e., days when discharge $> 90\%$ -tile) and compared these values to means derived for an equivalent number of days before and after the event.

All Bayesian analyses, regressions, and ANOVAs were performed using RStudio (R Core Team 2017). Days with negative GPP values constituted $< 6\%$ of all daily estimates and were not removed prior to derivation of monthly means

used for statistical analysis. ANOVA was used to partition variation in monthly average GPP and ER. For the longitudinal dataset, a three-way ANOVA was performed using segment, method, month, and their interaction terms. For the time series dataset (VCU Rice Pier), the three-way ANOVA included month, year, method, and their interaction terms. Linear regressions were performed to assess relationships between GPP and ER, between GPP and ER with water temperature, and between ecosystem and pelagic metabolism. Paired *t* tests were used to compare estuarine metabolism before, during, and after high discharge events. The GAM analysis of dissolved oxygen data was conducted using the “mgcv” package in R (Wood 2006; Beck and Murphy 2017). The package default thin plate regression spline was used to depict effect sizes of water level and temperature on DO; a cyclic cubic regression spline was used to depict diel (time of day) effects on DO (Wood 2006). Model results were scaled to center on the mean DO to assess the effect of each predictor variable.

Results

Advective Influences on Dissolved Oxygen

The Generalized Additive Models accounted for 37–66% of the variation in dissolved oxygen and revealed similar functional relationships with the three predictor variables (tidal stage, time of day, and water temperature) across all five salinity segments (Fig. 2). The largest effects on dissolved oxygen were associated with water temperature with a response range of 4–8 mg O₂ L⁻¹. These showed the expected negative relationship of decreasing oxygen with increasing water temperature, except at the high end of the temperature range (> 30 °C) where an increase in oxygen concentrations was detected by the non-linear models. Functional relationships with time of day (solar effects) exhibited the expected diel patterns with minimum and maximum values occurring at ~ 6 am and ~ 4 pm, respectively. Largest diel amplitudes were observed in the mesohaline (~ 3 mg L⁻¹), with smallest amplitudes (~ 1 mg L⁻¹) occurring in the upper tidal fresh segment. Advective influences were smaller in comparison to diel and temperature effects, except in the oligohaline where dissolved oxygen concentrations varied by ~ 4 mg L⁻¹ as a function of water elevation. The GAM analysis also detected small declines in dissolved oxygen (~ 2 mg L⁻¹) during unusually high water level conditions in the lower tidal fresh and mesohaline segments. To determine whether oxygen changes associated with tidal stage influenced our estimates of metabolism, we fit a linear regression to the functional relationship for the oligohaline ($R^2 = 0.99$) and used this relationship to generate stage-corrected dissolved oxygen data for the full (3-yr) time series. Advection-corrected metabolism estimates derived using the bookkeeping method were compared to similar

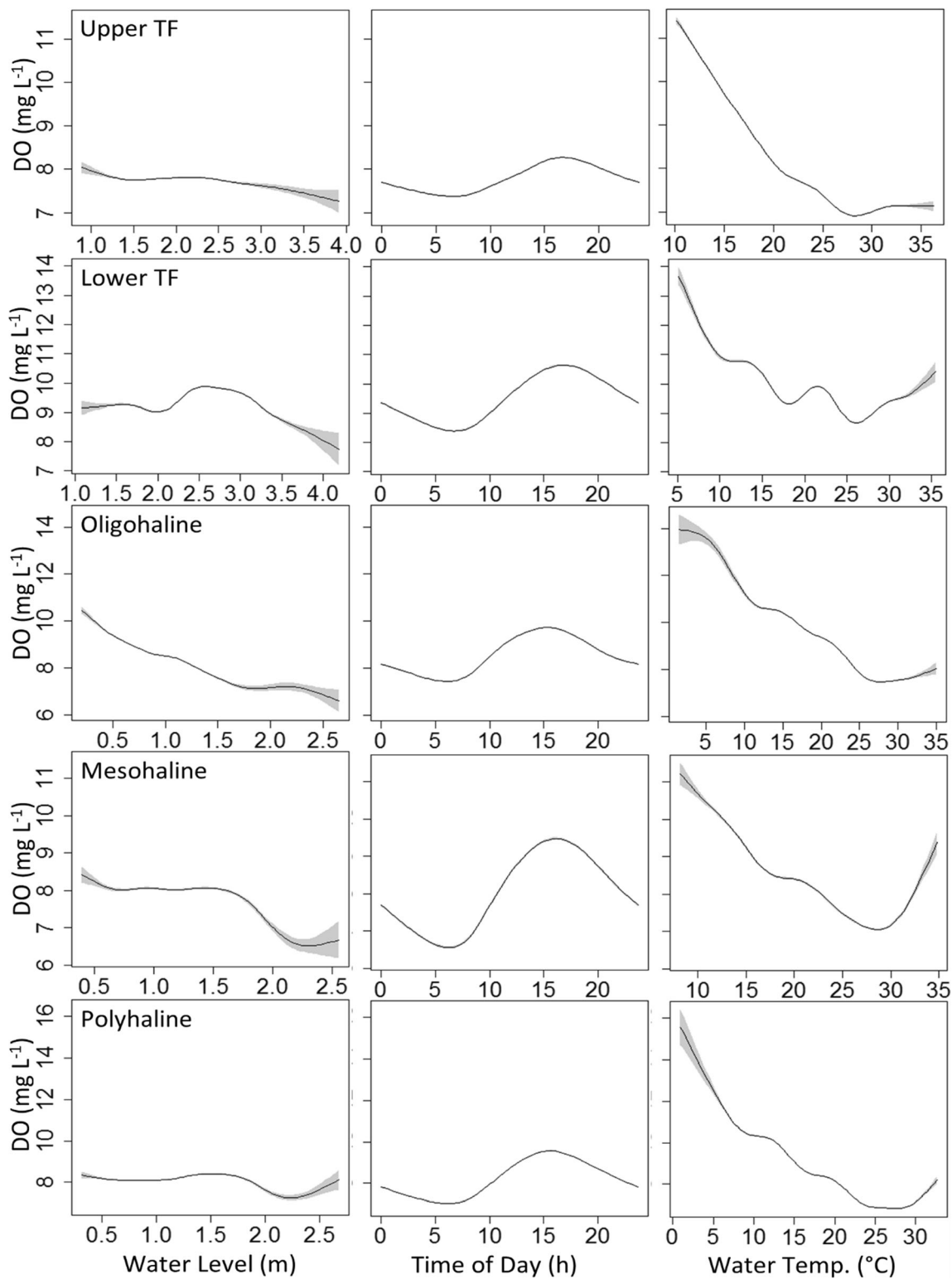


Fig. 2 Results from a Generalized Additive Model depicting functional relationships between dissolved oxygen and tidal stage (water level), time of day, and water temperature for five salinity segments of the James River Estuary

values from the original (uncorrected) dataset. Based on paired *t* tests, we found no statistically significant difference in GPP, ER, or AE between the two datasets, and therefore, we

concluded that advective oxygen fluxes did not affect our estimates of metabolism in this segment, or in other segments, where advective effects were weaker.

Longitudinal Comparisons

Data collected by the Chesapeake Bay Program were used to characterize longitudinal gradients in salinity, TSS, chlorophyll-*a* (CHL*a*), SAV, Secchi depth, and nutrient concentrations (TN, TP) during the time span for which metabolism estimates were derived (March–November 2007–2009;

Fig. 3). Freshwater dominated the estuary as indicated by low salinity (<5) extending over the upper 110 km (stations at river mile 42 to 110) and high salinity (>20) being restricted to the lower 10 km (stations 0–5). The estuarine turbidity maximum (ETM) extended over 70 km (stations 75 to 32) where median TSS concentrations were 15–25 mg L⁻¹. Median TSS was less than 10 mg L⁻¹ at stations above and

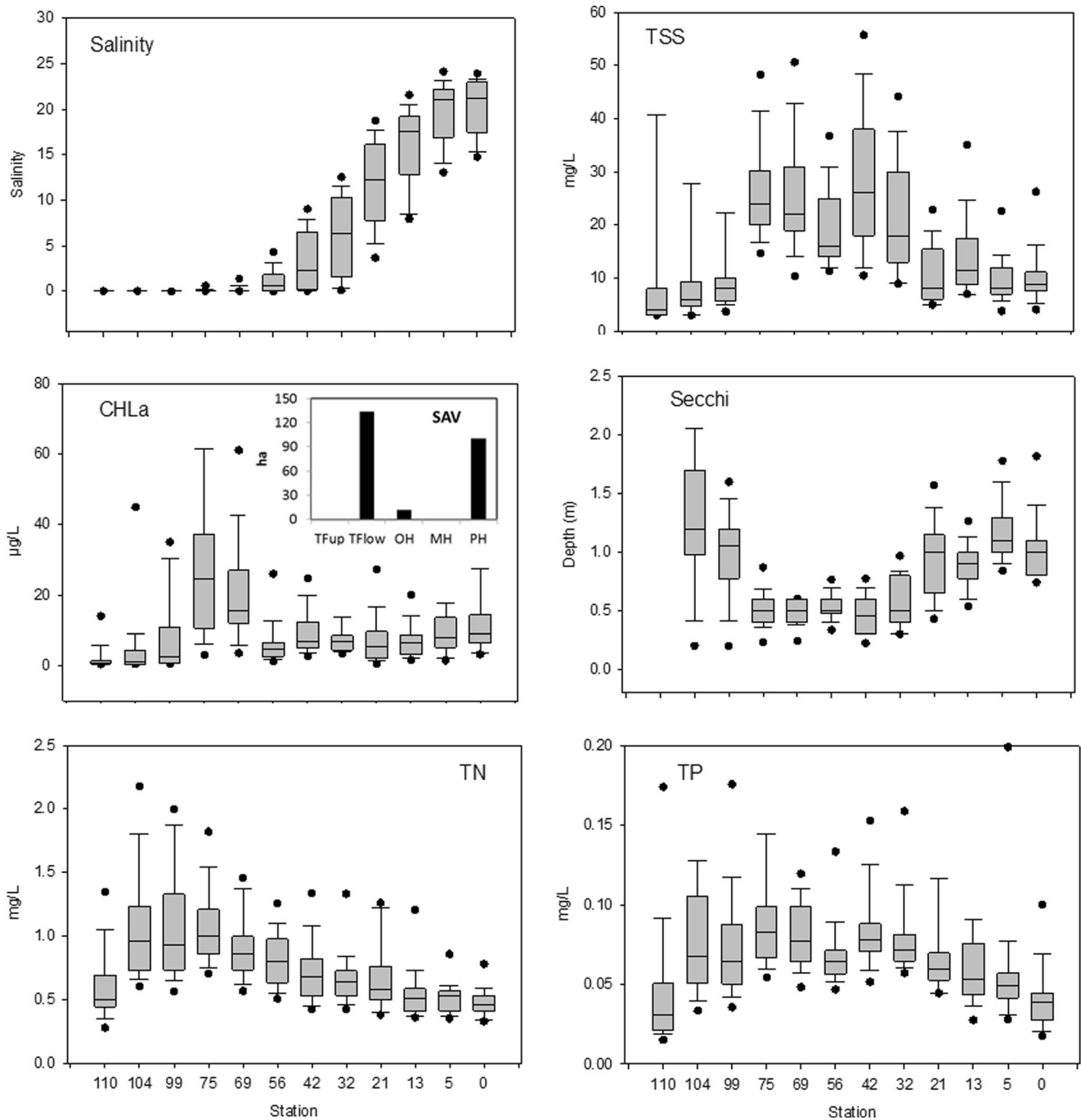


Fig. 3 Longitudinal patterns in salinity, total suspended solids (TSS), chlorophyll-*a* (CHL*a*), Secchi depth, TN, and TP in the James River Estuary (inset: SAV coverage by segment). Data are based on monthly Chesapeake Bay Program sampling for the time period corresponding to

measurements of estuarine metabolism (March–November 2007–2009). Station numbers correspond to distance in river miles from the confluence with Chesapeake Bay

below the ETM, though occasional values exceeding 100 mg L^{-1} were observed in the upper tidal fresh segment during high discharge events. There was a CHLa maximum in the lower tidal fresh segment (stations 75 and 69) where median concentrations were 25 and $16 \text{ } \mu\text{g L}^{-1}$ (respectively). Median CHLa was less than $10 \text{ } \mu\text{g L}^{-1}$ at all other stations. Highest SAV coverage was observed in the lower tidal fresh and polyhaline segments, which together comprised $> 90\%$ of total coverage in the estuary. Water clarity as indicated by Secchi depth was highest in the upper tidal fresh segment ($> 1 \text{ m}$), lowest within the ETM ($< 0.5 \text{ m}$), and intermediate ($\sim 1 \text{ m}$) seaward of the ETM. TN and TP concentrations were highest in the tidal fresh segments (median TN $\sim 1 \text{ mg L}^{-1}$, TP = 0.08 mg L^{-1}) and declined by 50% in the saline portion of the estuary.

The two methods of computation revealed similar patterns of increasing ER and GPP with salinity (Fig. 4 and Table 2). GPP increased by three- to fivefold from the upper tidal fresh segment to the polyhaline. ER tracked GPP and exhibited a similar range of values. Seaward increases in GPP were more than offset by increases in ER, resulting in increasingly

negative NEM along the longitudinal gradient. NEM was negative in four of the five salinity segments, with the exception of the lower tidal fresh. Positive NEM in the lower tidal fresh segment corresponded to negative values for atmospheric exchange, whereas all other segments exhibited positive fluxes (i.e., net gain from the atmosphere). Atmospheric exchange values were reflective of differences in oxygen saturation, which were typically super-saturated in the lower tidal fresh segment and under-saturated in all other segments. Median air-water fluxes for each segment were small ($< 2 \text{ g O}_2 \text{ m}^{-2} \text{ day}^{-1}$) in comparison to biologically driven oxygen fluxes (GPP and ER = 4 to $20 \text{ g O}_2 \text{ m}^{-2} \text{ day}^{-1}$).

Results from a three-way ANOVA showed that longitude (salinity segments) accounted for the greatest proportion of variation in both GPP and ER (45 and 58%, respectively; Table 3). Month accounted for the second largest proportion of variation in GPP and ER (23 and 17%, respectively). Method was also a significant factor, but its effects on GPP and ER varied by segment and month, as indicated by significant interaction effects. The proportion of variation explained by method inclusive of the main effect and interaction terms

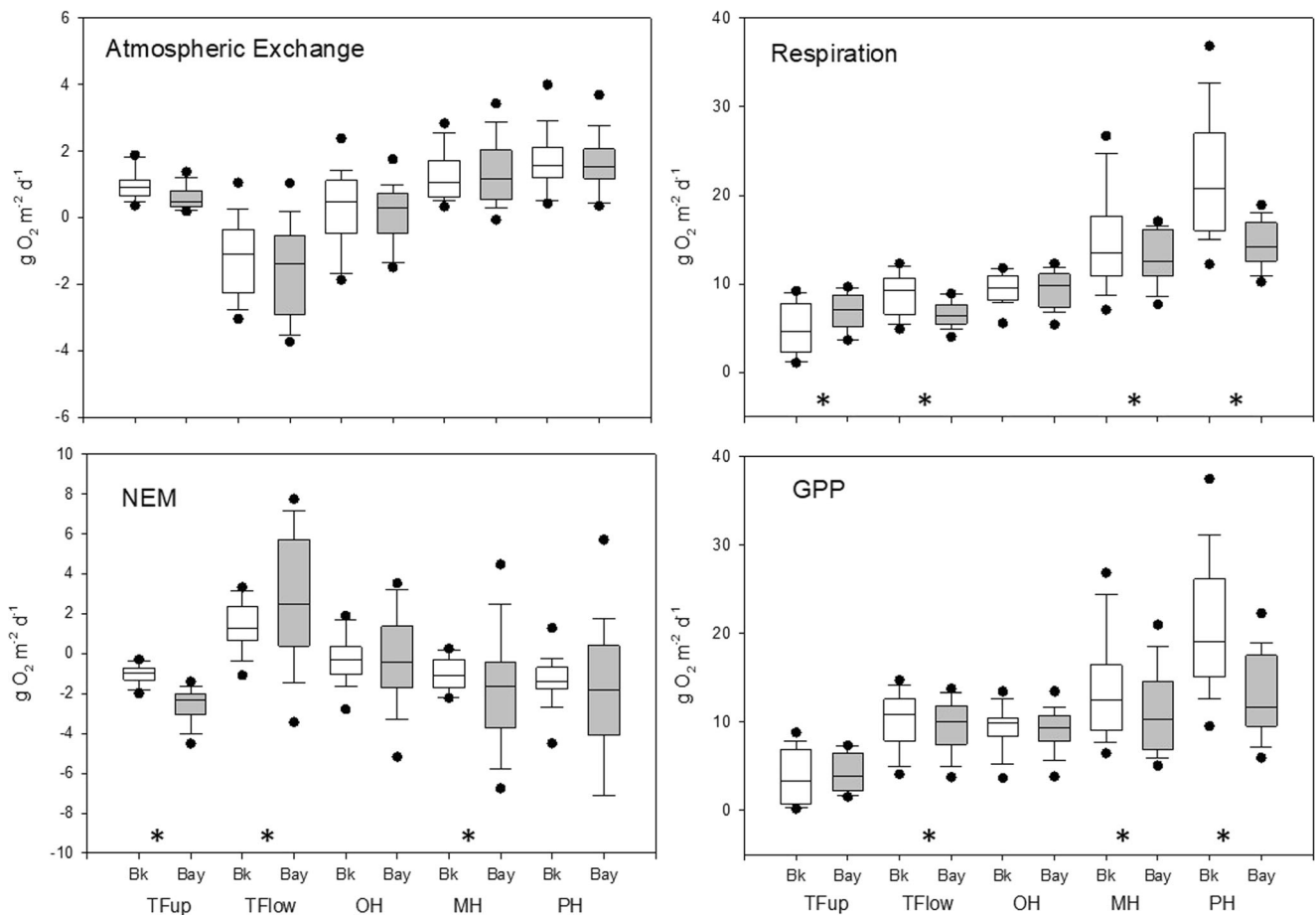


Fig. 4 Longitudinal patterns in atmospheric exchange, respiration, net ecosystem metabolism (NEM), and gross primary production (GPP) derived from diel oxygen data using bookkeeping (Bk) and Bayesian (Bay) methods (asterisks denote significant differences between methods)

Table 2 Areal estimates of atmospheric exchange (AE), ecosystem respiration (ER), net ecosystem metabolism (NEM), and gross primary production (GPP) derived by bookkeeping (BK) and Bayesian (Bay) methods for salinity segments of the James River Estuary

Segment	AE (g O ₂ m ⁻² day ⁻¹)		ER (g O ₂ m ⁻² day ⁻¹)		NEM (g O ₂ m ⁻² day ⁻¹)		GPP (g O ₂ m ⁻² day ⁻¹)	
	BK	Bay	BK	Bay	BK	Bay	BK	Bay
TF _{Upper}	0.99 ± 0.10	0.62 ± 0.08	4.86 ± 0.62	6.83 ± 0.44	-1.02 ± 0.11	-2.59 ± 0.19	3.84 ± 0.66	4.25 ± 0.46
TF _{Lower}	-1.23 ± 0.24	-1.61 ± 0.29	8.76 ± 0.49	6.63 ± 0.30	1.43 ± 0.25	2.84 ± 0.65	10.18 ± 0.65	9.47 ± 0.63
OH	0.23 ± 0.25	0.06 ± 0.19	9.56 ± 0.36	9.41 ± 0.43	-0.24 ± 0.27	-0.20 ± 0.51	9.32 ± 0.51	9.20 ± 0.51
MH	1.24 ± 0.16	1.34 ± 0.20	14.53 ± 1.14	12.95 ± 0.63	-0.98 ± 0.18	-1.87 ± 0.61	13.56 ± 1.20	11.08 ± 0.93
PH	1.71 ± 0.17	1.62 ± 0.17	22.07 ± 1.33	14.61 ± 0.50	-1.35 ± 0.24	-1.97 ± 0.73	20.71 ± 1.43	12.64 ± 0.89

Values are mean (± SE) for data collected during May–November 2006–2008

was 11% (GPP) and 12% (ER). The bookkeeping method yielded significantly higher estimates of GPP and ER for the lower tidal fresh, mesohaline, and polyhaline segments ($p < 0.02$, paired t test). The largest differences between the two methods were observed in the polyhaline, where GPP and ER were highest (Fig. 5). Bookkeeping estimates of GPP and ER for the polyhaline were ~ 8 g O₂ m⁻² day⁻¹ higher; corresponding to a difference of 64% (GPP) and 51% (ER) over Bayesian values. Among all other segments, bookkeeping values were 9% (GPP) and 6% (ER) higher relative to Bayesian values. Across all segments, there was a strong correlation between values derived by the two methods ($R^2 = 0.85$ and 0.73 for GPP and ER, respectively; $p < 0.001$). We did not find consistent differences between the two methods for estimates of NEM. The bookkeeping method yielded significantly lower estimates of NEM in the lower tidal fresh ($p = 0.001$) and higher estimates in the mesohaline ($p = 0.035$). The two methods yielded significantly different rates of atmospheric exchange in all five segments. However, absolute differences were small (mean difference = 0.18 ± 0.03 g O₂ m⁻² day⁻¹) and the paired estimates were highly correlated ($R^2 = 0.97$, $p < 0.001$). The slope of their relationship was near unity

(1.06 ± 0.02) with an intercept near zero (-0.22 ± 0.03) over a range of observed values from -3 to 5 g O₂ m⁻² day⁻¹.

Seasonal and Interannual Comparisons

For the 8-year time series from the lower tidal fresh segment, the two methods revealed similar seasonal and interannual patterns in metabolism. Highest monthly averages of GPP and ER were observed in summer when solar radiation and water temperature were highest (Fig. 6). Results from the three-way ANOVA showed that month accounted for the greatest proportion of variation in both GPP (73%) and ER (43%; Table 4). The strong patterns of seasonal variability were reflected in significant relationships between GPP and water temperature ($R^2 = 0.84$, $p < 0.0001$; both methods) and between ER and water temperature ($R^2 = 0.80$ and 0.29 , bookkeeping and Bayesian, respectively; both $p < 0.0001$). Year accounted for a significant but small (1%) proportion of the variation in ER but not GPP. Method did not account for a significant proportion of variation in GPP but accounted for 19% of variation in ER (inclusive of main and interactive effects). On average, the bookkeeping method yielded 30%

Table 3 Results from a three-way ANOVA testing the effect of salinity segment (Upper TF, Lower TF, OH, MH and PH), month, computational method (bookkeeping vs. Bayesian), and their interactions on monthly average values of GPP and ER from the James River Estuary

Variable	GPP					ER				
	Df	Sum Sq	F	R ²	p	Df	Sum Sq	F	R ²	p
Segment	4	4024	147.0	0.45	< 0.001	4	4895	278.3	0.58	< 0.001
Month	8	2079	38.0	0.23	< 0.001	8	1409	40.0	0.17	< 0.001
Method	1	352	51.5	0.04	< 0.001	1	265	60.3	0.03	< 0.001
Segment/method	4	603	22.0	0.07	< 0.001	4	603	34.3	0.07	< 0.001
Segment/month	26	695	3.9	0.08	< 0.001	26	308	2.7	0.04	< 0.001
Method/month	8	79	1.4	ns	0.18	8	193	5.5	0.02	< 0.001
Segment/method/month	26	60	0.3	ns	0.9	26	167	1.5	ns	0.08
Residuals	148	1013				148	651			
Total		8905		0.87			8491		0.90	

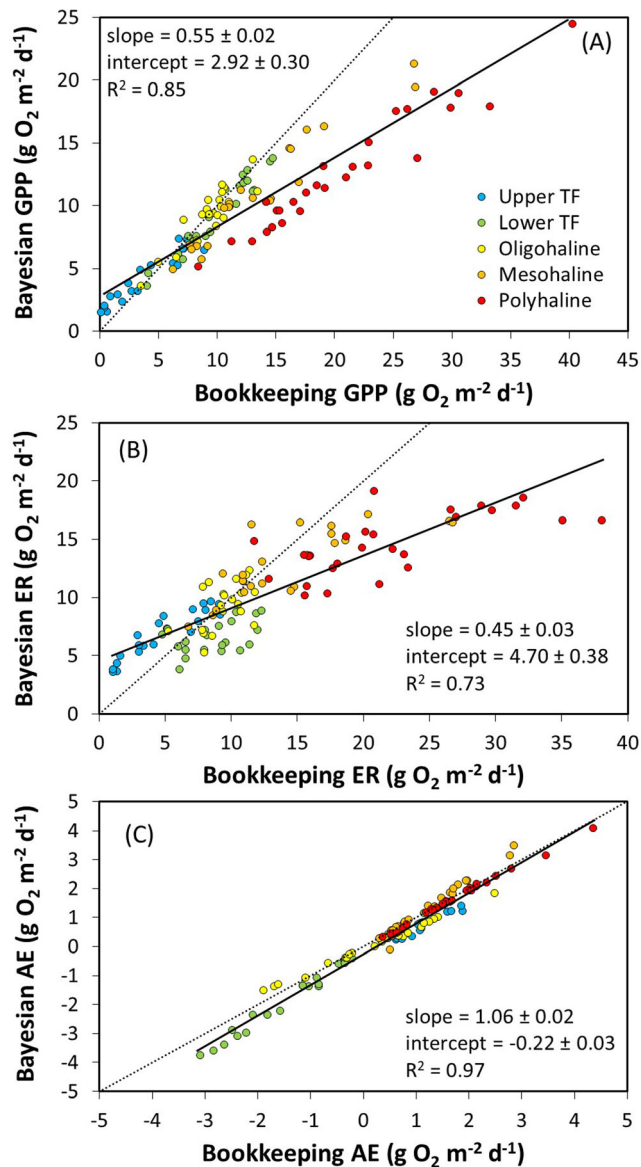


Fig. 5 Comparisons of bookkeeping and Bayesian estimates of GPP, ER, and atmospheric exchange (AE) among salinity segments of the James Estuary (all regressions $p < 0.0001$). Dotted lines represent 1:1 relationship

higher estimates of ER (mean difference = $1.35 \pm 0.35 \text{ g O}_2 \text{ m}^{-2} \text{ day}^{-1}$), whereas GPP differed by only 4% (mean difference = $0.26 \pm 0.12 \text{ g O}_2 \text{ m}^{-2} \text{ day}^{-1}$). We found strong correlations between the bookkeeping and Bayesian estimates for both GPP and atmospheric exchange ($R^2 = 0.93$ and 0.94 , respectively; $p < 0.001$) with slopes near unity and intercepts near zero. The relationship for ER was weaker ($R^2 = 0.25$, $p < 0.001$) and exhibited a slope less than 1 (0.40 ± 0.07).

The bookkeeping method yielded higher estimates of ER in the upper portion of the range. As higher ER was observed in summer, the bookkeeping results accentuated seasonal patterns relative to the Bayesian method, which yielded more similar values of ER over the annual cycle. This effect was

reflected in the significant method-by-month interaction term for the ER analysis. The bookkeeping estimates of ER varied by fivefold between summer (mean = $10.12 \pm 0.40 \text{ g O}_2 \text{ m}^{-2} \text{ day}^{-1}$) and winter (mean = $1.96 \pm 0.21 \text{ g O}_2 \text{ m}^{-2} \text{ day}^{-1}$), whereas Bayesian estimates differed by less than twofold between summer (mean = $5.94 \pm 0.69 \text{ g O}_2 \text{ m}^{-2} \text{ day}^{-1}$) and winter (mean = $3.69 \pm 0.34 \text{ g O}_2 \text{ m}^{-2} \text{ day}^{-1}$). As the bookkeeping method yielded higher values of ER, estimates of NEM were 68% lower (mean difference = $-0.92 \pm 0.26 \text{ g O}_2 \text{ m}^{-2} \text{ day}^{-1}$) relative to Bayesian values.

The two methods revealed similar patterns of interannual variation in GPP with highest annual means in 2010 and 2012 and lowest in 2009 (Fig. 7). The grand mean of GPP and range of annual means was similar for the two methods (bookkeeping = $6.29 \text{ g O}_2 \text{ m}^{-2} \text{ day}^{-1}$, interannual CV = 14%; Bayesian = $6.03 \text{ g O}_2 \text{ m}^{-2} \text{ day}^{-1}$, interannual CV = 18%). The Bayesian method yielded a lower estimate of mean ER with greater interannual variability ($4.51 \text{ g O}_2 \text{ m}^{-2} \text{ day}^{-1}$, interannual CV = 31%) relative to the bookkeeping method ($5.86 \text{ g O}_2 \text{ m}^{-2} \text{ day}^{-1}$, interannual CV = 11%). Annual mean ER derived by the two methods differed by as much as $2 \text{ g O}_2 \text{ m}^{-2} \text{ day}^{-1}$ in some years (2009, 2015, 2016). On average, Bayesian estimates of annual NEM were $1.09 \text{ g O}_2 \text{ m}^{-2} \text{ day}^{-1}$ higher than bookkeeping values, though differences were variable from year-to-year in magnitude and direction (range = -0.48 to $2.80 \text{ g O}_2 \text{ m}^{-2} \text{ day}^{-1}$). Despite this, the two methods showed consistent agreement in annual net C balance of the tidal fresh segment for 7 of 8 years. Both methods indicated net autotrophy during 2010–2014 and net heterotrophy in 2009 and 2015. We did not find coherent patterns between interannual variation in GPP and ER with solar radiation, water temperature, CHLa, SAV, discharge or inputs of nutrients, and organic matter. For example, GPP was unusually low in 2009 (20 and 36% below 8-year average based on bookkeeping and Bayesian estimates, respectively) despite favorable conditions as indicated by above average solar radiation (+10%), below average discharge (−54%), and above average nutrient inputs (DIN = +22%, PO₄ = +41%). In 2013, we observed above average hydrologic (+88%) and organic matter inputs (POC = +92%, DOC = +77%) and below average CHLa (−26%), whereas GPP and ER were within 15% of the 8-year average (both methods). Unusually low SAV abundance in 2016 (80% below average) was accompanied by near-normal GPP (within 10% of average).

Ecosystem and Pelagic Metabolism

Over an annual cycle, pelagic GPP and R averaged 4.77 ± 0.50 and $3.32 \pm 0.41 \text{ g O}_2 \text{ m}^{-2} \text{ day}^{-1}$ (respectively) in the tidal fresh segment of the James. Highest rates were observed in summer months (June–September: GPP = 5 – $9 \text{ g O}_2 \text{ m}^{-2} \text{ day}^{-1}$, R = 3 – $6 \text{ g O}_2 \text{ m}^{-2} \text{ day}^{-1}$), whereas in October–May, GPP was $< 4 \text{ g O}_2 \text{ m}^{-2} \text{ day}^{-1}$ and R was $< 3 \text{ g O}_2 \text{ m}^{-2}$

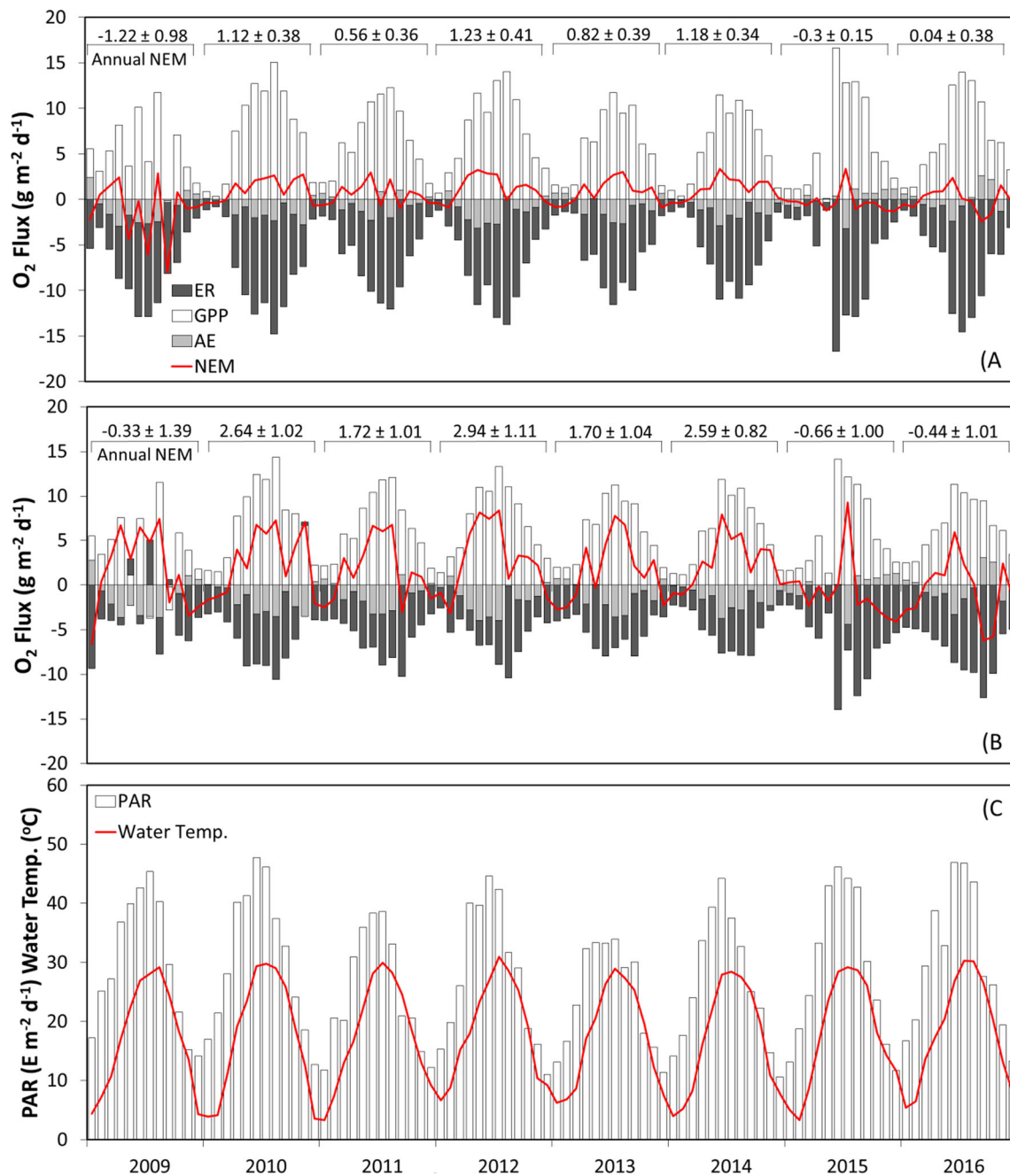


Fig. 6 Monthly averages of daily ecosystem respiration (ER), gross primary production (GPP), atmospheric exchange (AE), and net ecosystem metabolism (NEM) in the lower tidal fresh segment derived

by the bookkeeping (a) and Bayesian methods (b). Also shown (c) are monthly mean solar radiation and water temperature for this station

day⁻¹. Ecosystem GPP and R were significantly correlated with pelagic GPP and R (Fig. 8). Bookkeeping estimates yielded stronger correlations with pelagic GPP ($R^2 = 0.74$) and ER ($R^2 = 0.62$; both $p < 0.0001$) relative to Bayesian estimates (GPP: $R^2 = 0.47$, $p < 0.0001$; ER: $R^2 = 0.18$, $p = 0.03$). Pelagic GPP was equivalent to $66 \pm 3\%$ (bookkeeping) and $68 \pm 6\%$ (Bayesian) of annual ecosystem GPP during 2009–2016. Pelagic R was equivalent to $47 \pm 2\%$ (bookkeeping) and $44 \pm 2\%$ (Bayesian) of annual ER during this period.

Relationships Between ER and GPP

We compared the relationships between ER and GPP for values derived from the longitudinal and time series datasets using both computational methods (Fig. 9). For the longitudinal dataset (all segments), the bookkeeping estimates showed a stronger correlation ($R^2 = 0.96$) between ER and GPP than the Bayesian estimates ($R^2 = 0.46$; $p < 0.001$ for both). For the time series dataset (VCU RRC pier), we also found a stronger

Table 4 Results from a three-way ANOVA testing the effect of month, year, computational method (bookkeeping vs. Bayesian), and their interactions on monthly average values of GPP and ER for an 8-year times series from the tidal fresh segment of the James River Estuary

Variable	GPP					ER				
	Df	Sum Sq	F	R ²	p	Df	Sum Sq	F	R ²	p
Month	11	2412	47.5	0.73	<0.001	11	965	19.5	0.43	<0.001
Year	1	0.3	0.1	ns	0.81	1	30	6.8	0.01	0.01
Method	1	3	0.7	ns	0.40	1	87	19.4	0.04	<0.001
Year/method	1	2	0.3	ns	0.57	1	55	12.3	0.02	<0.001
Year/month	11	173	3.4	0.05	<0.001	11	109	2.2	0.05	0.017
Method/month	11	25	0.5	ns	0.91	11	294	5.9	0.13	<0.001
Year/method/month	11	6	0.1	ns	1.00	11	40	0.8	ns	0.63
Residuals	144	665				144	647			
Total		3284		0.79			2227		0.69	

relationship for the bookkeeping estimates ($R^2 = 0.83$) relative to the Bayesian estimates ($R^2 = 0.19$; $p < 0.001$ for both). The intercept of this relationship was used to infer allochthonous contributions to ecosystem respiration (i.e., ER at GPP = 0; del Giorgio and Peters 1994). For the longitudinal dataset, the Bayesian results yielded a significantly higher intercept (4.52 ± 0.06 g O₂ m⁻² day⁻¹) relative to the bookkeeping method (0.58 ± 0.02 g O₂ m⁻² day⁻¹). When compared to corresponding average values of ER (bookkeeping = 12.49 ± 0.71 g O₂ m⁻² day⁻¹; Bayesian = 10.32 ± 0.38 g O₂ m⁻² day⁻¹), the proportion of respiration attributed to allochthonous inputs was 5% (bookkeeping) and 44% (Bayesian). For the time series dataset, Bayesian results also yielded a significantly higher intercept (2.52 ± 0.50 g O₂ m⁻² day⁻¹) relative to the bookkeeping method (1.01 ± 0.28 g O₂ m⁻² day⁻¹). When compared to the corresponding average values of ER (bookkeeping = 5.86 ± 0.38 g O₂ m⁻² day⁻¹; Bayesian = 4.51 ± 0.30 g O₂ m⁻² day⁻¹), the proportion of respiration attributed to allochthonous inputs was 17% (bookkeeping) and 56% (Bayesian).

High Discharge Events

We examined the effect of high discharge events on estuarine metabolism using bookkeeping estimates derived from the time series (lower tidal fresh) dataset. For the period from January 2009 to December 2014, there were 28 events during which daily discharge exceeded 90%-tile values for at least three consecutive days (average length = 5.6 day). The average discharge during events was 847 m³ s⁻¹; corresponding pre- and post-event values were 304 and 359 m³ s⁻¹. When water temperature exceeded 14 °C (14 events), GPP and ER were significantly lower during events in comparison to pre-event conditions (paired *t* test, $p < 0.001$ for both; Fig. 10). Comparable declines were observed for both GPP (by 43% from 7.81 ± 1.08 to 4.48 ± 0.89 g O₂ m⁻² day⁻¹) and ER (by 36% from 7.07 ± 0.99 to 4.51 ± 0.72 g O₂ m⁻² day⁻¹). Post-

event GPP and ER were not significantly different from pre-event values ($p = 0.28$ and 0.29 , respectively). For events occurring during low water temperature (< 14 °C), there was no significant change in GPP or ER prior to vs. during the event ($p = 0.19$ and 0.14 , respectively).

Discussion

Comparison of Computational Methods

Our analysis of diel oxygen data from the James River estuary showed that differences in GPP, ER, and atmospheric exchange derived by two commonly used computational methods were small in comparison to seasonal, longitudinal, and interannual variability. Estimating atmospheric exchange was of particular concern as prior empirical studies (e.g., using propane injection in streams) have shown high variability even under similar hydrologic conditions (Bott et al. 2006). Recent work using eddy covariance techniques at riverine sites showed that variability in oxygen exchange can arise from small, transient temperature gradients at the air-water interface (Berg and Pace 2017). In our study, we used two approaches that differed in their level of parameterization but yielded similar results. The simpler method used in the bookkeeping analysis assumed that atmospheric exchange was influenced only by oxygen gradients at the air-water boundary (i.e., dissolved oxygen saturation), whereas the more complex method used local wind data and estimates of water velocity from a hydrodynamic model as priors for the Bayesian analysis. The average difference between the two methods was small (0.18 ± 0.03 g O₂ m⁻² day⁻¹) in relation to the range of derived values (-3 to 5 g O₂ m⁻² day⁻¹). Although the two methods yielded good precision, we are unable to assess their accuracy in the absence of empirical measurements of AE for the James. Raymond and Cole (2001) compiled empirical and modeled

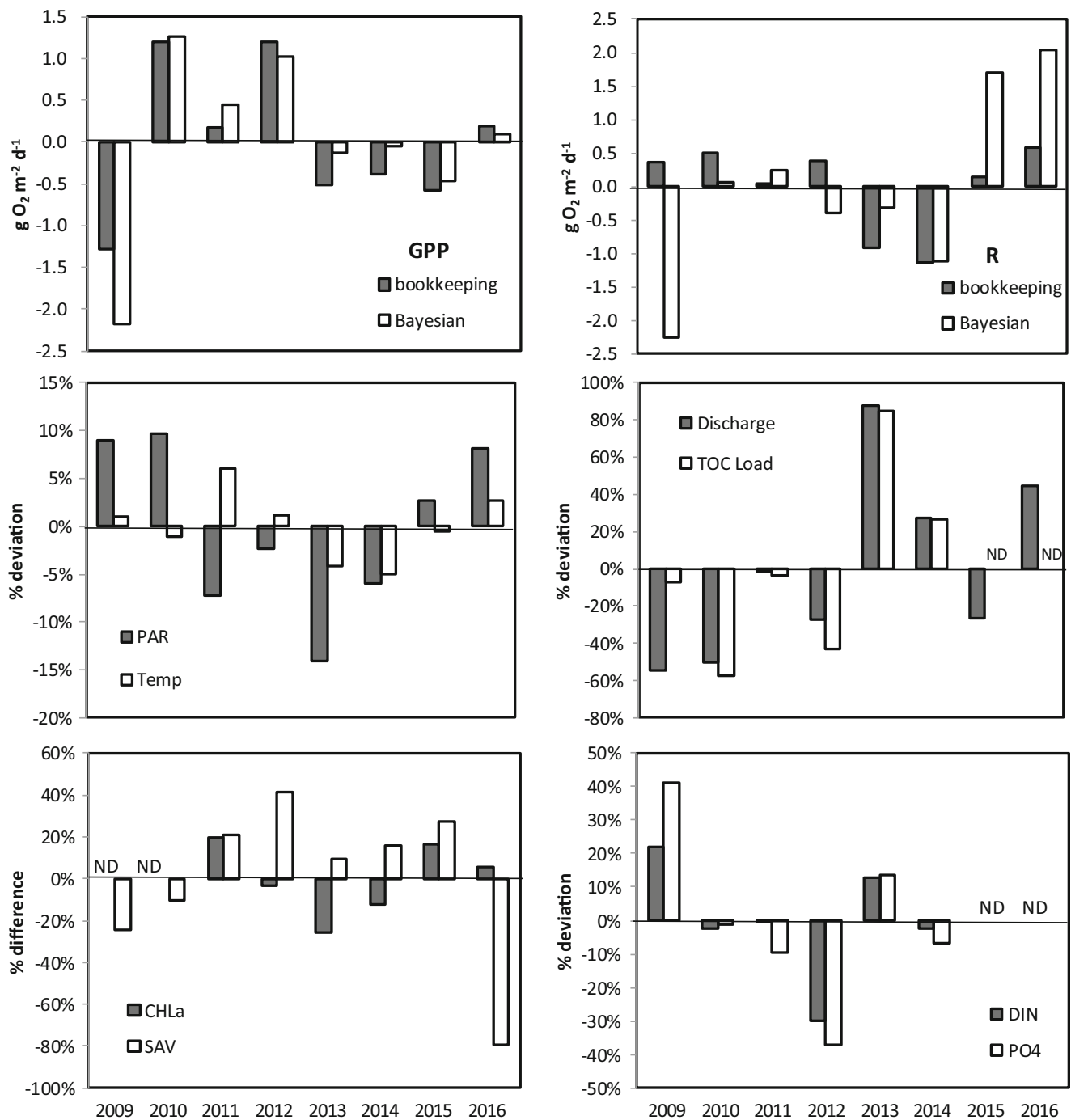


Fig. 7 Interannual variation in estuarine GPP and R (bookkeeping and Bayesian estimates), solar radiation, water temperature, discharge, TOC inputs, chlorophyll-*a* (CHLa), SAV, and nutrient inputs. Data shown are

deviations from the 8-year average as absolute (GPP and R) or relative (%) values (all other). Inputs of water, TOC, and nutrients are for May to September of each year

estimates of gas transfer velocities for estuaries and concluded that expected k_{600} values should be in the range of 3–7 $cm h^{-1}$. Our segment-specific values fell within this range (3.8 to 6.2 $cm h^{-1}$). The low rates of atmospheric exchange relative to biotic fluxes, and the small difference between methods, suggest that for this system, estimation of GPP and ER should be relatively robust with respect to uncertainty in AE. In estuaries, the

influence of atmospheric exchange on oxygen budgets may be smaller (relative to streams and small rivers) due to their greater depth (lower surface area to volume ratio) and higher rates of biologically driven oxygen fluxes (Hoellein et al. 2013; Murrell et al. 2018).

Our results also show that advective oxygen fluxes had little effect on estimates of metabolism for this estuary.

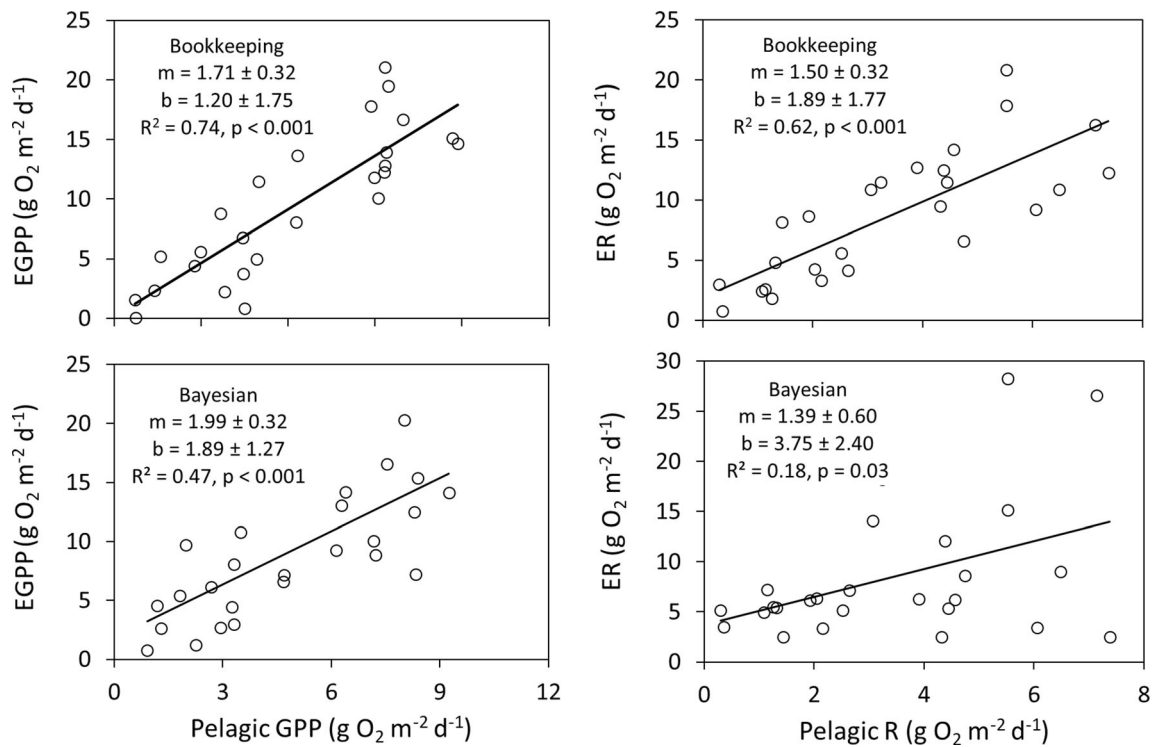


Fig. 8 Relationships between pelagic GPP and R with ecosystem GPP and R (EGPP and ER, respectively) derived by bookkeeping and Bayesian methods (m = slope, b = intercept). Data were collected over an annual cycle at stations located in the tidal freshwater segment of the James River Estuary

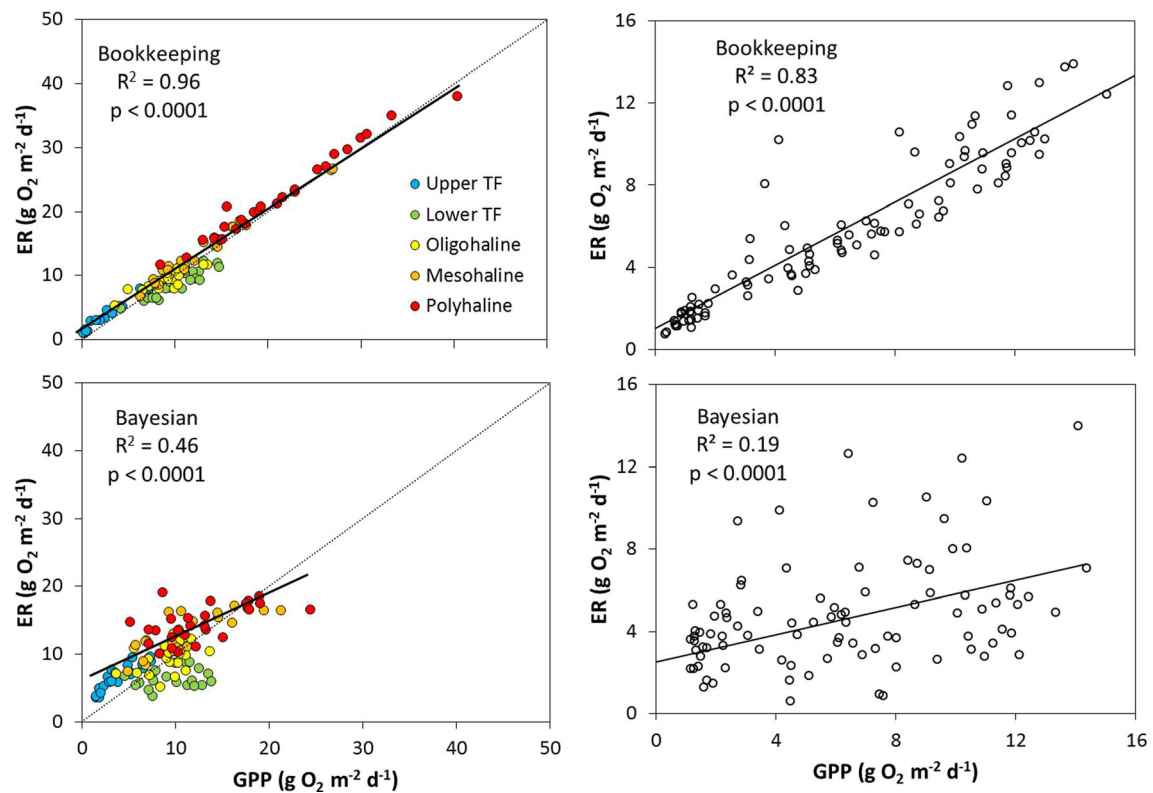


Fig. 9 Relationships between monthly average ER and GPP for the longitudinal (left) and time series (right) datasets derived using bookkeeping and Bayesian computational methods

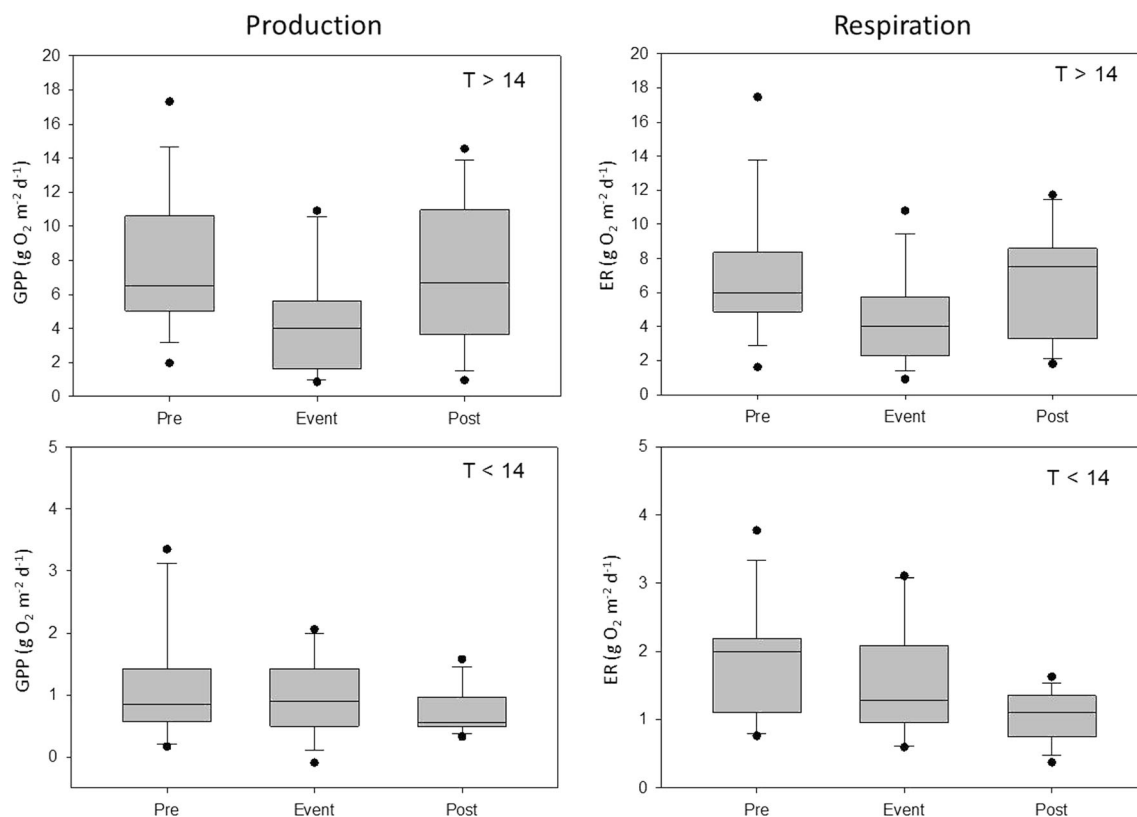


Fig. 10 Influence of high discharge events on estuarine metabolism (bookkeeping estimates) as indicated by median values of GPP and ER before, during, and after events. Events occurring during high ($> 14\text{ }^{\circ}\text{C}$) and low ($< 14\text{ }^{\circ}\text{C}$) water temperature were analyzed separately

Functional relationships between dissolved oxygen and tidal stage (GAM results) showed generally flat responses across the range of water elevations. The oligohaline segment was an exception, where we observed higher oxygen concentrations at low water level. We attribute this to the influence of the lower tidal fresh segment where oxygen concentrations were typically super-saturated. During an outgoing tide, oxygen-rich water from the lower tidal fresh segment would raise oxygen in the oligohaline, whereas during an incoming tide, this oxygen-rich water would be replaced by lower oxygen waters from lower estuary. Despite this influence, we found no statistically detectable difference between monthly averaged metabolism estimates derived with and without correction for advective effects.

We found generally good agreement for estimates of GPP and ER derived by the two methods. Statistical analyses showed that computational method accounted for a small proportion of the variation in GPP and ER in comparison to that accounted for by seasonal and longitudinal variables. For the tidal fresh time series, bookkeeping estimates of GPP were on average 4% higher (by $0.26 \pm 0.12\text{ g O}_2\text{ m}^{-2}\text{ day}^{-1}$) relative to Bayesian values. For the longitudinal dataset, bookkeeping estimates of GPP were 26% higher ($2.50 \pm 0.36\text{ g O}_2\text{ m}^{-2}\text{ day}^{-1}$). These differences were small in comparison to the range of variation observed in the time series (1.4 to $10.6\text{ g O}_2\text{ m}^{-2}\text{ day}^{-1}$) and longitudinal (3.5 to $22.6\text{ g O}_2\text{ m}^{-2}\text{ day}^{-1}$; 10th and 90th percentile values) datasets.

For ER, bookkeeping estimates were 30% higher ($2.50 \pm 0.36\text{ g O}_2\text{ m}^{-2}\text{ day}^{-1}$) for the tidal fresh time series and 21% higher ($2.17 \pm 0.44\text{ g O}_2\text{ m}^{-2}\text{ day}^{-1}$) for the longitudinal dataset over a similar range of values. By contrast, Cloern et al. (2014) reported a large range of variation (threefold) among estimates of phytoplankton production derived by various methods, though this encompassed not only computational differences, but also methodology (e.g., oxygen- vs. radiocarbon-based estimates). Aristegi et al. (2009) reported that estimates of GPP and ER for Spanish streams varied by fivefold depending on the computational method used.

Methodological influences on estimation of estuarine metabolism varied by segment and season. This pattern arose because the bookkeeping method yielded higher estimates of GPP and ER in the upper end of the range, and smaller estimates in the lower end of the range, thereby resulting in a broader range of seasonal and longitudinal values. We do not have a mechanistic explanation for why the Bayesian method yielded a smaller range of values, but note that Bayesian estimates were lower than bookkeeping estimates in the range of values above the prior and higher in the range of values below the prior. This suggests that the specification of priors influenced the outcome of the Bayesian analysis. The priors used in this study were from bookkeeping estimates of metabolism for six mid-Atlantic estuaries (14 station-years of data) encompassing a range of salinities from tidal fresh to

polyhaline (Caffrey 2003, 2004). Given the proximity of these sites, we consider that these priors were well-suited for use in the Bayesian analysis of James River data. Our findings suggest that inferences regarding spatial and temporal patterns in metabolism were robust with respect to computational methodology but that monthly average values may differ by as much as 60% at the high end of the range (e.g., polyhaline GPP and ER).

Seasonal, Longitudinal, and Interannual Patterns

Seasonal cycles in water temperature and solar radiation impact estuarine metabolism, with greatest GPP and ER during summer and lowest rates in winter (Cory 1974; Boynton et al. 1982; Cole et al. 1992; D'Avanzo et al. 1996; Testa et al. 2012; Caffrey et al. 2014). In the James, seasonal variation in estuarine GPP and ER followed expected patterns related to water temperature and solar radiation, with large (three- to fivefold) differences between winter and summer months. Interannual differences were small by comparison. Coefficients of variation among annual mean GPP and ER were 14 and 11% (respectively) for the 8-year time series from the tidal fresh segment. Interannual variation in estuarine productivity is often attributed to variation in river discharge and nutrient loads (Jassby et al. 2002), but we did not find that interannual differences in GPP and ER could be explained by riverine discharge or loads. For example, unusually high riverine discharge during May–September 2013 (+88%) was associated with low CHLa (−26%), whereas GPP was only 8% below average. Similarly, we did not find that interannual differences in GPP or ER tracked variation in annual or summer loads of nutrients or organic matter. Interannual variation in the abundance of grazers is a potential driver of ecosystem GPP in phytoplankton-dominated systems (Jassby et al. 2002; Strayer et al. 2008). Our prior work has shown that rotifers, planktivorous fishes, and wedge clams (*Rangia*) are the dominant grazers in this system (Wood et al. 2016), but we lack long-term data to assess their role in affecting interannual variation in estuarine metabolism.

Prior studies have shown that longitudinal variation in salinity and channel morphometry influences GPP and ER (Boynton et al. 1982; Kemp et al. 1997; Sellers and Bukaveckas 2003; Paerl et al. 2010; Roelke et al. 2017) and the balance between heterotrophy and autotrophy (Smith and Kemp 1995; Kemp et al. 1997; Raymond et al. 2000; Caffrey 2004). We observed increasing areal GPP and ER with increasing salinity in the James. Increasing depth only partially accounts for greater areal ER as depth increased by twofold along the longitudinal gradient, whereas ER increased by fourfold. Longitudinal patterns in GPP did not track SAV coverage, which was highest in the Tidal Fresh and Polyhaline segments. These findings suggest that SAV is not a major driver of ecosystem production in this estuary. Moore et al. (2000) estimated the biomass of Chesapeake Bay freshwater

and saline (*Zostera*-dominated) SAV communities to be 1.31 and 1.24 metric tons (dry mass) per hectare (respectively). Assuming this to represent the annual net SAV production, and a C content equivalent to 50% of dry mass, we estimate SAV NPP as 1.53 and 0.81 g C m^{−2} year^{−1} for the Lower Tidal Fresh and Polyhaline segments (respectively) based on areal SAV coverage for 2007–2009. Corresponding ecosystem estimates of NEP were 1340 and 2400 g C m^{−2} year^{−1} (respectively). The small contribution from SAV reflects their limited coverage (~1% of area for Tidal Fresh and Polyhaline segments) and the relatively low production within SAV beds (~65 g C m^{−2} year^{−1}) relative to water column production (see below).

Prior studies have reported greater heterotrophy in the upper, freshwater portions of estuaries (Kemp et al. 1997; Raymond et al. 2000; Caffrey 2004; Gazeau et al. 2005; Tomaso and Najjar 2015). For the James, we found a correspondence between the location of the CHLa maximum and the occurrence of net autotrophy in the tidal fresh segment. Favorable light conditions and longer water residence time foster the accumulation of phytoplankton biomass in the lower portion of the tidal fresh segment (Shen and Lin 2006; Bukaveckas et al. 2011). Despite the limited photic depth (~2 m), shallow areas lateral to the main channel provide favorable light conditions due to the low ratio of photic-to-total depth. The partial release from light limitation enhances phytoplankton utilization of nutrient inputs from riverine and local point sources (Wood and Bukaveckas 2014). Annualized estimates of phytoplankton production for the Lower Tidal Fresh segment (NPP = 750 g C m^{−2} year^{−1}; GPP = 1170 g C m^{−2} year^{−1}) fall at the high end of the range (upper 10%-tile) among data for 131 estuaries compiled by Cloern et al. (2014). The excess of production over respiration within the water column likely accounts for positive ecosystem NEM. Our data show that pelagic production accounts for ~65% of ecosystem production, indicating that benthic and epiphytic algae may contribute a third of primary production in the tidal fresh segment.

Riverine inputs affect estuarine metabolism through advective transport of phyto- and bacterio-plankton and indirectly through loading of nutrients and organic matter (Paerl et al. 2010; Bruesewitz et al. 2013; Caffrey et al. 2014; Cloern et al. 2014). We found that during high discharge events, ecosystem production and respiration declined by 43 and 36% (respectively) but that recovery to baseline (pre-event) values occurred within a time span of days. Our findings suggest that estuaries dominated by pelagic production may be more resilient in comparison to streams and rivers where scouring events reduce the biomass of benthic autotrophs (Bernhardt et al. 2018). The response of heterotrophs to high discharge events may depend in part on the quality and quantity of OM delivered to the estuary. Zwart et al. (2017) reported a positive effect of storm-driven OM inputs on lake metabolism. We did

not observe this response in the James, which is surprising given that the tidal fresh segment retains a large proportion of POC inputs (Bukaveckas et al. 2018). Stable isotope analysis showed that suspended and sedimented particulate matter in the James was predominantly of allochthonous origin (Wood et al. 2016), as would be expected for an estuary with a large watershed area (Sakamaki et al. 2010). Stable isotopes also indicate that the bulk of metazoan production in the tidal fresh segment is supported by allochthonous inputs due to detritivory by adult gizzard shad and benthic filter-feeders (*Rangia* clams). For the upper James, we can conclude that allochthonous inputs are important as a bulk flux of OM, and for food web energetics, but we were unable to reliably estimate the proportion of ER that was supported by internal vs. external sources. The lack of response to variation in OM inputs, and the positive OM balance (net autotrophy) for this segment, suggests that allochthonous inputs may be largely sequestered (buried). Our further work in this system seeks to better understand the fate of C inputs.

Cross-System Comparisons

A meta-analysis of diel oxygen-based metabolism data by Hoellein et al. (2013) showed that estuaries have twofold higher metabolism ($GPP \sim 10 \text{ g O}_2 \text{ m}^{-2} \text{ day}^{-1}$; $ER \sim 13 \text{ g O}_2 \text{ m}^{-2} \text{ day}^{-1}$) relative to streams, wetlands, and lakes. Our area-weighted (by salinity segment) bookkeeping values for a corresponding time period (June–August) were above the estuarine average for both GPP (range of means for 2006–2008 = $14.6\text{--}17.4 \text{ g O}_2 \text{ m}^{-2} \text{ day}^{-1}$) and ER ($15.4\text{--}17.9 \text{ g O}_2 \text{ m}^{-2} \text{ day}^{-1}$). High rates of production and respiration in estuaries are attributed to external inputs of OM and nutrients from riverine and, in some cases, marine sources (Vincent et al. 1996; Kemp et al. 1997; Muylaert et al. 2005; Hoellein et al. 2013). Nutrient inputs elevate primary production thereby providing labile OM, which is supplemented by allochthonous OM inputs. The James receives high loads of organic matter inputs from its large and forested catchment, as well as labile nutrients in wastewater from major metropolitan areas located in the tidal fresh and polyhaline segments (Bukaveckas and Isenberg 2013; Bukaveckas et al. 2018). The combined effects of nutrient and organic matter inputs may in part account for elevated rates of metabolism observed in this system, relative to other estuaries.

Hoellein et al. (2013) reported stronger correlations between GPP and ER in estuaries relative to other aquatic systems. For the James, we observed strong correlations between GPP and ER among bookkeeping-based estimates. The strong coupling suggests that GPP provides labile sources of OM to support ER, and re-mineralization of organic matter provides nutrients to support GPP. The prevalence of net heterotrophic conditions indicates that allochthonous inputs support respiration in excess of OM supply via autochthonous production.

Among the 48 estuaries included in the meta-analysis, 11% were net autotrophic and 89% were net heterotrophic (Hoellein et al. 2013). In the James, area-weighted NEM was negative over the 3-year period when data for all segments were available (range of annual means = -0.43 to $-0.85 \text{ g O}_2 \text{ m}^{-2} \text{ day}^{-1}$). Net autotrophy was observed only in the lower tidal fresh segment, which accounted for a relative small proportion ($< 10\%$) of total area. Our efforts to assess the importance of allochthonous contributions (based on ER at $GPP = 0$) produced conflicting results as the bookkeeping method yielded a small intercept relative to the mean (i.e., low allochthony), whereas the Bayesian method indicated near-equal importance of autochthonous and allochthonous OM sources. Bayesian estimates yielded weaker relationships between GPP and ER and therefore greater uncertainty in estimates of ER at $GPP = 0$. The weaker coupling among estimates derived by inverse modeling has also been observed for lakes and attributed to the fact that bookkeeping estimates of GPP are not determined independently from estimates of ER ($GPP = \text{daytime NEP}$; Obrador et al. 2014).

Conclusions

Components of metabolism, particularly primary production, are commonly measured in estuaries, but few studies provide sufficiently comprehensive data that span gradients of salinity and over multiple years (Cloern et al. 2014). We analyzed a large number of dissolved oxygen measurements ($\sim 800,000$) from the James River Estuary to better understand seasonal, interannual, and longitudinal patterns in metabolism. We found that seasonal patterns closely tracked water temperature and solar radiation, whereas longitudinal and interannual patterns were less readily interpretable based on knowledge of the distribution of primary producers and variation in riverine inputs of nutrients and organic matter. With increasing ease of collecting continuous monitoring data, large datasets will become more widely available, thereby increasing the need to standardize the processing of these data for cross-system comparisons (Oczkowski et al. 2016; Murrell et al. 2018). Our study shows that the method used to derive metabolic estimates can impact some aspects interpretation, such as sources of OM supporting metabolism. A simplified version of the bookkeeping approach that used fixed estimates of atmospheric exchange yielded generally similar results to those derived by a Bayesian inverse modeling approach with variable atmospheric exchange. These findings suggest that in the absence of ancillary data on wind and water velocity, estuarine metabolism can be reliably estimated using a fixed exchange coefficient. The bookkeeping approach required minimal parameterization, was computationally easier, and provided generally similar results, though with a broader range of values that accentuated seasonal and longitudinal differences. We hope these findings will shed light on how various computational

approaches may influence estimation of estuarine metabolism from diel oxygen data and the robustness of inferences drawn from these results.

Acknowledgements We are grateful to our colleagues at the Virginia Institute of Marine Science for making the longitudinal diel oxygen dataset available via their VECOS website and to the Virginia Department of Environmental Quality Piedmont and Tidewater Offices for collecting longitudinal water quality data. We thank Alison Appling (USGS) for her assistance with the Bayesian modeling and Jian Shen (VIMS) for providing model output on atmospheric exchange coefficients for the James. Ken Moore and Robert Orth (VIMS) provided data and helpful discussions on SAV. Three anonymous reviewers provided valuable comments. This paper is a contribution to the VCU Rice Rivers Center.

References

- Appling, A. P., R. O. Hall, M. Arroita, and C. B. Yackulic. 2017. streamMetabolizer: models for estimating aquatic photosynthesis and respiration. R package version 0.9.33. <https://github.com/USGS-R/streamMetabolizer>.
- Aristegi, L., O. Izagirre, and A. Elosegi. 2009. Comparison of several methods to calculate reaeration in streams and their effects on estimation of metabolism. *Hydrobiologia* 635 (1): 113–124.
- Beck, M.W., and R.R. Murphy. 2017. Numerical and qualitative contrasts of two statistical models for water quality change in tidal waters. *Journal of the American Water Resources Association* 53 (1): 197–219.
- Berg, P., and M.L. Pace. 2017. Continuous measurement of air-water gas exchange by underwater eddy covariance. *Biogeosciences* 14 (23): 5595–5606.
- Bernhardt, E.S., J.B. Heffernan, N.B. Grimm, E.H. Stanley, J.W. Harvey, et al. 2018. The metabolic regimes of flowing waters. *Limnology and Oceanography* 63: 99–118.
- Borges, A.V. 2005. Do we have enough pieces of the jigsaw to integrate CO₂ fluxes in the coastal ocean? *Estuaries and Coasts* 28 (1): 3–27.
- Bott, T.L., D.S. Montgomery, J.D. Newbold, D.B. Arscott, C.L. Dow, A.K. Aufdenkampe, J.K. Jackson, and L.A. Kaplan. 2006. Ecosystem metabolism in streams of the Catskill Mountains (Delaware and Hudson River watersheds) and Lower Hudson Valley. *Journal of the North American Benthological Society* 25 (4): 1018–1044.
- Boynton, W., W. Kemp, and C. Keefe. 1982. *Estuarine comparisons: a comparative analysis of nutrients and other factors influencing estuarine phytoplankton production*. Estuarine comparisons. New York: Academic.
- Bricker, S., B. Longstaff, W. Dennison, A. Jones, K. Boicourt, C. Wicks, and J. Woerner. 2007. *Effects of nutrient enrichment in the nation's estuaries: a decade of change*. Silver Spring: NOAA Coastal Ocean Program Decision Analysis (Series 26) National Centers for Coastal Ocean Science.
- Bruesewitz, D.A., W.S. Gardner, R.F. Mooney, L. Pollard, and E.J. Buskey. 2013. Estuarine ecosystem function response to flood and drought in a shallow, semiarid estuary: nitrogen cycling and ecosystem metabolism. *Limnology and Oceanography* 58 (6): 2293–2309.
- Bukaveckas, P.A., and W.N. Isenberg. 2013. Loading, transformation and retention of nitrogen and phosphorus in the tidal freshwater James River (Virginia). *Estuaries and Coasts* 36 (6): 1219–1236.
- Bukaveckas, P.A., L.E. Barry, M.J. Beckwith, V. David, and B. Lederer. 2011. Factors determining the location of the chlorophyll maximum and the fate of algal production within the tidal freshwater James River. *Estuaries and Coasts* 34 (3): 569–582.
- Bukaveckas, P.A., M. Beck, D. Devore, and W.M. Lee. 2018. Climatic variability and its role in regulating C, N and P retention in the James River Estuary. *Estuarine, Coastal and Shelf Science* 205: 161–173.
- Caffrey, J.M. 2003. Production, respiration and net ecosystem metabolism in U.S. estuaries. *Environmental Monitoring and Assessment* 81 (1): 207–219.
- Caffrey, J.M. 2004. Factors controlling net ecosystem metabolism in U.S. estuaries. *Estuaries and Coasts* 27 (1): 90–101.
- Caffrey, J.M., M.C. Murrell, K.S. Amacker, J.W. Harper, S. Phipps, and M.S. Woodrey. 2014. Seasonal and inter-annual patterns in primary production, respiration, and net ecosystem metabolism in three estuaries in the northeast Gulf of Mexico. *Estuaries and Coasts* 37 (S1): 222–241.
- Carignan, R., A. Blais, and C. Vis. 1998. Measurement of primary production and community respiration in oligotrophic lakes using the Winkler method. *Canadian Journal of Fisheries and Aquatic Sciences* 55 (5): 1078–1084.
- Cloern, J.E., S. Foster, and A. Kleckner. 2014. Phytoplankton primary production in the world's estuarine-coastal ecosystems. *Biogeosciences* 11 (9): 2477–2501.
- Cole, J.J., N.F. Caraco, and B.L. Peierls. 1992. Can phytoplankton maintain a positive carbon balance in a turbid, freshwater, tidal estuary? *Limnology and Oceanography* 37 (8): 1608–1617.
- Cole, J.J., M.L. Pace, S.R. Carpenter, and J.F. Kitchell. 2000. Persistence of net heterotrophy in lakes during nutrient addition and food web manipulations. *Limnology and Oceanography* 45 (8): 1718–1730.
- Collins, J.R., P.A. Raymond, W.F. Bohlen, and M.M. Howard-Strobel. 2013. Estimates of new and total productivity in Central Long Island Sound from in situ measurements of nitrate and dissolved oxygen. *Estuaries and Coasts* 36 (1): 74–97.
- Cory, R. 1974. Changes in oxygen and primary production of the Patuxent estuary, Maryland, 1963 through 1969. *Chesapeake Science* 15 (2): 78–83.
- Crosswell, J.R., M.S. Wetz, B. Hales, and H.W. Paerl. 2012. Air-water CO₂ fluxes in the microtidal Neuse River Estuary, North Carolina. *Journal of Geophysical Research: Oceans* 117 (C8).
- D'Avanzo, C., J.N. Kremer, and S.C. Wainright. 1996. Ecosystem production and respiration in response to eutrophication in shallow temperate estuaries. *Marine Ecology Progress Series* 4 (44): 263–274.
- Deacon, E. 1981. Sea-air gas transfer: the wind speed dependence. *Boundary-Layer Meteorology* 21 (1): 31–37.
- del Giorgio, P.A., and R.H. Peters. 1994. Patterns in planktonic P:R ratios in lakes: influence of lake trophy and dissolved organic carbon. *Limnology and Oceanography* 39 (4): 772–787.
- Gazeau, F., J. Gattuso, J.J. Middelburg, N. Brion, L. Schiettecatte, M. Frankignoulle, et al. 2005. Planktonic and whole system metabolism in a nutrient-rich estuary (the Scheldt Estuary). *Estuaries and Coasts* 28 (6): 868–883.
- Grace, M.R., D.P. Giling, S. Hladysz, V. Caron, R.M. Thompson, and R. Mac Nally. 2015. Fast processing of diel oxygen curves: Estimating stream metabolism with BASE (BAYesian Single-station estimation). *Limnology and Oceanography: Methods* 13 (3): 103–114.
- Hall, R.O., J.L. Tank, M.A. Baker, E.J. Rosi-Marshall, and E.R. Hotchkiss. 2016. Metabolism, gas exchange, and carbon spiraling in rivers. *Ecosystems* 19 (1): 73–86.
- Herrmann, M., R. Najjar, W.M. Kemp, R.B. Alexander, E.W. Boyer, W.-J. Cai, P.C. Griffith, K.D. Kroeger, S.L. McCallister, and R.A. Smith. 2015. Net ecosystem production and organic carbon balance of U.S. East Coast estuaries: a synthesis approach. *Global Biogeochemical Cycles* 29 (1): 96–111.
- Ho, D.T., P. Schlosser, and P.M. Orton. 2011. On factors controlling air-water gas exchange in a large tidal river. *Estuaries and Coast* 34 (6): 1103–1116.
- Hobbs, N.T., and M.B. Hooten. 2015. *Bayesian models: a statistical primer for ecologists*. Princeton: Princeton University Press.

- Hoellein, T.J., D.A. Bruesewitz, and D.C. Richardson. 2013. Revisiting Odum (1956): a synthesis of aquatic ecosystem metabolism. *Limnology and Oceanography* 58 (6): 2089–2100.
- Holtgrieve, G.W., D.E. Schindler, T.A. Branch, and Z.T. A'mar. 2010. Simultaneous quantification of aquatic ecosystem metabolism and reaeration using a Bayesian statistical model of oxygen dynamics. *Limnology and Oceanography* 55 (3): 1047–1063.
- Hopkinson, C., and E.M. Smith. 2005. Estuarine respiration: an overview of benthic, pelagic, and whole system respiration. In *Respiration in aquatic ecosystems*, 122–146. New York: Academic.
- Houser, J.N., L.A. Bartsch, W.B. Richardson, J.T. Rogala, and J.F. Sullivan. 2015. Ecosystem metabolism and nutrient dynamics in the main channel and backwaters of the upper Mississippi River. *Freshwater Biology* 60 (9): 1863–1879.
- Jähne, B., K.O. Münnich, R. Börsinger, A. Dutzi, W. Huber, and P. Libner. 1987. On the parameters influencing air-water gas exchange. *Journal of Geophysical Research: Oceans* 92 (C2): 1937–1949.
- Jassby, A.D., J.E. Cloern, and B.E. Cole. 2002. Annual primary production: patterns and mechanisms of change in a nutrient-rich tidal ecosystem. *Limnology and Oceanography* 47 (3): 698–712.
- Kemp, W., E. Smith, M. Marvin-DiPasquale, and W. Boynton. 1997. Organic carbon balance and net ecosystem metabolism in Chesapeake Bay. *Marine Ecology Progress Series* 150: 229–248.
- Lindeman, R.L. 1942. The trophic-dynamic aspect of ecology. *Ecology* 23 (4): 399–417.
- Moore, K.A., D. Wilcox, and R.J. Orth. 2000. Analysis of the abundance of submersed aquatic vegetation communities in Chesapeake Bay. *Estuaries* 23 (1): 115–127.
- Morton, R., and B.L. Henderson. 2008. Estimation of non-linear trends in water quality: an improved approach using generalized additive models. *Water Resources Research* 44 (7): W07420.
- Murrell, M.C., J.M. Caffrey, D.T. Marcovich, M.W. Beck, B.M. Jarvis, and J.D. Hagy. 2018. Seasonal oxygen dynamics in a warm temperate estuary: effects of hydrologic variability on measurements of primary production, respiration and net metabolism. *Estuaries and Coasts* 41 (3): 690–707.
- Muyllaert, K., M. Tackx, and W. Vyverman. 2005. Phytoplankton growth rates in the freshwater tidal reaches of the Schelde Estuary (Belgium) estimated using a simple light-limited primary production model. *Hydrobiologia* 540 (1-3): 127–140.
- O'Connor, D., and W. Dobbins. 1958. Mechanism of reaeration in natural streams. *Transactions of the American Society of Civil Engineers* 123: 641–684.
- Obrador, B., P.A. Staehr, and J.P.C. Christensen. 2014. Vertical patterns of metabolism in three contrasting stratified lakes. *Limnology and Oceanography* 59 (4): 1228–1240.
- Oczkowski, A., C.W. Hunt, M. Miller, C.A. Oviatt, S.W. Nixon, and L. Smith. 2016. Comparing measures of estuarine ecosystem production in a temperate New England estuary. *Estuaries and Coasts* 39 (6): 1827–1844.
- Odum, H.T. 1956. Primary production in flowing waters. *Limnology and Oceanography* 1 (2): 102–117.
- Paerl, H.W., K.L. Rossignol, S.N. Hall, B.L. Peierls, and M.S. Wetz. 2010. Phytoplankton community indicators of short-and long-term ecological change in the anthropogenically and climatically impacted Neuse River Estuary, North Carolina, USA. *Estuaries and Coasts* 33 (2): 485–497.
- R Core Team. 2017. *R: a language and environment for statistical computing*. Vienna: R Foundation for Statistical Computing <https://www.R-project.org/>.
- Raymond, P.A., and J.J. Cole. 2001. Gas exchange in rivers and estuaries: choosing a gas transfer velocity. *Estuaries* 24 (2): 312–317.
- Raymond, P.A., J.E. Bauer, and J.J. Cole. 2000. Atmospheric CO₂ evasion, dissolved inorganic carbon production, and net heterotrophy in the York River Estuary. *Limnology and Oceanography* 45 (8): 1707–1717.
- Raymond, P.A., C.J. Zappa, D. Butman, T.L. Bott, J. Potter, P. Mulholland, et al. 2012. Scaling the gas transfer velocity and hydraulic geometry in streams and small rivers. *Limnology and Oceanography: Fluids and Environments* 2: 41–53.
- Raymond, P.A., J. Hartmann, R. Lauerwald, S. Sobek, C. McDonald, M. Hoover, D. Butman, R. Striegl, E. Mayorga, C. Humborg, P. Kortelainen, H. Dürr, M. Meybeck, P. Ciais, and P. Guth. 2013. Global carbon dioxide emissions from inland waters. *Nature* 503 (7476): 355–359.
- Richards, R., L. Hughes, D. Gee, and R. Tomlinson. 2013. Using generalized additive models for water quality assessments: a case study example from Australia. *Journal of Coastal Research* 65: 111–116.
- Roelke, D.L., H. Li, C.J. Miller-DeBoer, G.M. Gable, and S.E. Davis. 2017. Regional shifts in phytoplankton succession and primary productivity in the San Antonio bay system (USA) in response to diminished freshwater inflows. *Marine and Freshwater Research* 68 (1): 131–145.
- Sakamaki, T., J.Y.T. Shum, and J.S. Richardson. 2010. Watershed effects on chemical properties of sediment and primary consumption in estuarine tidal flats: Importance of watershed size and food selectivity by macrobenthos. *Ecosystems* 11: 328–337.
- Sellers, T., and P.A. Bukaveckas. 2003. Phytoplankton production in a large, regulated river: a modeling and mass balance assessment. *Limnology and Oceanography* 48 (4): 1476–1487.
- Shen, J., and J. Lin. 2006. Modeling study of the influences of tide and stratification on age of water in the tidal James River. *Estuarine, Coastal and Shelf Science* 68 (1-2): 101–112.
- Shen, J., Y. Wang, and M. Sisson. 2016. Development of the hydrodynamic model for long-term simulation of water quality processes of the tidal James River, Virginia. *Journal of Marine Science and Engineering* 4 (4): 82.
- Smith, E.M., and W.M. Kemp. 1995. Seasonal and regional variations in plankton community production and respiration for Chesapeake Bay. *Marine Ecology Progress Series* 116 (1): 217–231.
- Solomon, C.T., D.A. Bruesewitz, D.C. Richardson, K.C. Rose, M.C. Van de Bogert, P.C. Hanson, et al. 2013. Ecosystem respiration: drivers of daily variability and background respiration in lakes around the globe. *Limnology and Oceanography* 58 (3): 849–866.
- Staehr, P.A., J.M. Testa, W.M. Kemp, J.J. Cole, K. Sand-Jensen, and S.V. Smith. 2012. The metabolism of aquatic ecosystems: history, applications, and future challenges. *Aquatic Sciences* 74 (1): 15–29.
- Strayer, D.L., M.L. Pace, N.F. Caraco, J.J. Cole, and S.E.G. Findlay. 2008. Hydrology and grazing jointly control a large-river food web. *Ecology* 89 (1): 12–18.
- Testa, J.M., W.M. Kemp, C.S. Hopkinson, and S.V. Smith. 2012. Ecosystem metabolism. In *In estuarine ecology 381–416*. Hoboken: Wiley-Blackwell.
- Thomann, R.V., and J.A. Mueller. 1987. *Principles of surface water quality modeling and control*. New York: Harper & Row.
- Tomaso, D.J., and R.G. Najjar. 2015. Long-term variations in the dissolved oxygen budget of an urbanized tidal river: the upper Delaware Estuary. *Journal of Geophysical Research Biogeosciences* 120 (6): 1027–1045.
- Tranvik, L.J., J.A. Downing, J.B. Cotner, S.A. Loiselle, R.G. Striegl, T.J. Ballatore, P. Dillon, K. Finlay, K. Fortino, L.B. Knoll, P.L. Kortelainen, T. Kutser, S. Larsen, I. Laurion, D.M. Leech, S.L. McCallister, D.M. McKnight, J.M. Melack, E. Overholt, J.A. Porter, Y. Prairie, W.H. Renwick, F. Roland, B.S. Sherman, D.W. Schindler, S. Sobek, A. Tremblay, M.J. Vanni, A.M. Verschoor, E. von Wachenfeldt, G.A. Weyhenmeyer, et al. 2009. Lakes and reservoirs as regulators of carbon cycling and climate. *Limnology and Oceanography* 54 (6.2): 2298–2314.
- USEPA and Region III Chesapeake Bay Program Office. 2005. Chesapeake Bay program analytical segmentation scheme: revisions, decisions and rationales 1983–2003, 2005 addendum. *Rep.*

- No. EPA 903-R-05-004, Monitoring and Analysis Subcommittee, and Tidal Monitoring and Analysis Workgroup, Annapolis, Md.
- Vannote, R.L., G.W. Minshall, K.W. Cummins, J.R. Sedell, and C.E. Cushing. 1980. The river continuum concept. *Canadian Journal of Fisheries and Aquatic Sciences* 37 (1): 130–137.
- Vincent, W.F., J.J. Dodson, N. Bertrand, and J. Frenette. 1996. Photosynthetic and bacterial production gradients in a larval fish nursery: the St. Lawrence River transition zone. *Marine Ecology Progress Series* 139: 227–238.
- Wanninkhof, R. 1992. Relationship between wind speed and gas exchange over the ocean. *Journal of Geophysical Research: Oceans* 97 (C5): 7373–7382.
- Winslow, L.A., J.A. Zwart, R.D. Batt, H.A. Dugan, R.I. Woolway, J.R. Corman, P.C. Hanson, and J.S. Read. 2016. LakeMetabolizer: an R package for estimating lake metabolism from free-water oxygen using diverse statistical models. *Inland Waters* 6 (4): 622–636.
- Wood, S.N. 2006. *Generalized additive models: an introduction with R*. London: Chapman and Hall CRC Press.
- Wood, J.D., and P.A. Bukaveckas. 2014. Increasing severity of phytoplankton nutrient limitation following reductions in point source inputs to the tidal freshwater segment of the James River Estuary. *Estuaries and Coasts* 37 (5): 1188–1201.
- Wood, J.D., D. Elliott, G. Garman, D. Hopler, W. Lee, S. McNinch, A.J. Porter, and P.A. Bukaveckas. 2016. Autochthony, allochthony and the role of consumers in influencing the sensitivity of aquatic systems to nutrient enrichment. *Food Webs* 7: 1–12.
- Zwart, J.A., S.D. Sebestyen, C.T. Solomon, and S.E. Jones. 2017. The influence of hydrologic residence time on lake carbon cycling dynamics following extreme precipitation events. *Ecosystems* 20 (5): 1000–1014.